H3K27me3 is dispensable for early differentiation but required to maintain differentiated cell identity

Sara A. Miller[1,2], Manashree Damle[1], Robert E. Kingston[1,2,*]

AFFILIATIONS:

[1]Department of Molecular Biology, Massachusetts General Hospital Research Institute, Massachusetts General Hospital, Boston, Massachusetts 02114, USA

[2]Department of Genetics, Harvard Medical School, Boston, Massachusetts 02115, USA

*Correspondence: kingston@molbio.mgh.harvard.edu

Abstract

Polycomb repressive complex 2 (PRC2) catalyzes trimethylation of histone H3 on lysine 27 and is required for normal development of complex eukaryotes. The requirement for H3K27me3 in various aspects of mammalian differentiation is not clear. Though associated with repressed genes, the modification is not sufficient to induce gene repression, and in some instances is not required. To examine the role of the modification in mammalian differentiation, we blocked trimethylation of H3K27 with both a small molecule inhibitor, GSK343, and by introducing a point mutation into EZH2, the catalytic subunit of PRC2. We found that cells with substantively decreased H3K27 tri-methylation were able to differentiate, which contrasts with EZH2 null cells. Different PRC2 targets had varied requirements for H3K27me3 in repressive regulation with a subset that maintained normal levels of repression in the absence of methylation. The primary cellular phenotype when H3K27 tri-methylation was blocked was an inability of the altered cells to maintain a differentiated state when challenged. This phenotype was determined by H3K27me3 deposition both in embryonic stem cells and in the first four days of differentiation. H3K27 tri-methylation therefore was not necessary for formation of differentiated cell states but was required to maintain a stable differentiated state.

Introduction

Polycomb repressive complex 2 (PRC2) is a highly conserved protein complex that is required for proper axial patterning of vertebrates. It is comprised of the core subunits EZH2, SUZ12, EED and RBAP48, with additional subunits some of which are cell-type or developmental stage specific (Healy et al., 2019; Margueron & Reinberg, 2011; Shen et al., 2009; van Mierlo et al., 2019). The complex is crucial for differentiation, but it is not required for the self-renewing phenotype associated with embryonic stem (ES) cells (Aloia et al., 2013; Chamberlain et al.,

2008). At a molecular level, PRC2 family complexes are the only histone 3 lysine 27 (H3K27) methyltransferases identified in mammals. EZH2 is the primary catalytic component of these complexes, with its paralog EZH1 also contributing to catalytic activity in some instances (Margueron et al., 2008; Shen et al., 2008; Wassef et al., 2019; Xu et al., 2015). Lysine residues can be mono- di- or tri- methylated, with PRC2 able to catalyze all levels of methylation. Increased methylation is generally associated with gene repression, and H3K27 tri-methylation (H3K27me3) is a key marker of facultative heterochromatin. However, the tri-methylation of H3K27 is neither required nor sufficient to induce gene repression (Ahmed et al., 2018; Chamberlain et al., 2008; Ferguson et al., 2018; O'Geen et al., 2017). Dissecting the role of tri-methylated H3K27 in gene regulation is important for understanding how genes become repressed during development and retain their repression in differentiated cells.

Expression levels of Polycomb complexes have developmental and disease effects. Both hyper-activating and inactivating mutations in PRC2 have been identified from a variety of human cancers (Basheer et al., 2019; Cyrus et al., 2019; Jain & Di Croce, 2016). Malignancies with both types of alterations to PRC2 function have been linked to cancer progression and poor prognosis in a wide variety of tissue (Abdel Raouf et al., 2019; Basheer et al., 2019; Bohm et al., 2019; Bremer et al., 2019; Deng et al., 2019; Dou et al., 2019; Karlowee et al., 2019; Krill et al., 2020; Matsubara et al., 2019; Mechaal et al., 2019; Shi et al., 2019; Tian et al., 2019; Wasenang et al., 2019; M. J. Zhang et al., 2019; Q. Zhang et al., 2019). These findings are consistent with the initial identification of Polycomb-Group genes in Drosophila where haploinsufficiency yielded developmental phenotypes (Lewis & Mislove, 1947; Schuettengruber et al., 2017). Inserting these disease mutations into cells alters the modification profiles of H3K27 and can change their developmental potential. Increased methylation can often push cells toward a neuro progenitor phenotype (Juan et al., 2016; Pasini et al., 2007; Thornton et al., 2014). In cancer patients, increased levels of expression of PRC2 components and especially EZH2 leads to hypermethylation and is associated with poor prognosis (Tian et al., 2019; Wu et al., 2019). Consequently, there is significant interest in targeting this complex pharmaceutically. Small molecules that inhibit PRC2 methyltransferase activity have been approved for clinical trials (Fioravanti et al., 2018; Kondo, 2014; Liu et al., 2015; Lue & Amengual, 2018; Qi et al., 2012; Shi et al., 2019; Xu et al., 2015; Yamagishi & Uchimaru, 2017; Yang et al., 2019). It remains, however, unclear how far this activity can be manipulated before risking adverse effects from having too little of the modification present. The ambiguity of the role of H3K27me3 in disease progression increases the importance of understanding the mechanisms by which PRC2 methylation activities regulate gene expression during development.

Previous work on PRC2 has shown that the complex is dispensable for the propagation of self-renewing, undifferentiated cells that are phenotypically indistinguishable from WT ES cells. These studies have also shown that PRC2 deficient cells do not differentiate properly (Chamberlain et al., 2008; Lavarone et al., 2019; Pasini et al., 2007; Pasini et al., 2004; Shen et al., 2008). Since the entire complex is disrupted when any of the core components are knocked out, it is not clear whether it is solely the lack of methylation that is causing these developmental defects, or whether there are other mechanistic roles PRC2 plays that are distinct from methylation(Collinson et al., 2016; Rai et al., 2013; Shan et al., 2017; Yu et al.,

2017). A recent study examined the impact of a mutation in *Ezh2* that blocks all levels of methylation. When these cells were differentiated into embryoid bodies they showed visual phenotypic differences (Lavarone et al., 2019), demonstrating that complete removal of the methyltransferase activity of PRC2 impairs normal differentiation. We focus here on the developmental phenotypes caused by specific loss of the H3K27me3 modification, as opposed to loss of all methylation.

To determine the contribution that H3K27me3 makes to gene repression, we examined cells with a point mutation within the SET domain of *Ezh2* that generates a hypomorph that is predominately defective in tri-methylation. We also analyzed cells treated with a small molecule inhibitor that blocks tri-methylation more efficiently than di-methylation. The expression level of PRC2 has known effects on gene regulation, so we used strategies that do not impact the protein level or complex integrity, thus allowing a focus on methyltransferase activity. There are multiple small molecules that interrupt PRC2 methyltransferase activity both for research and current clinical trials; we used GSK343 (Bradley et al., 2014; Fraineau et al., 2017; Liu et al., 2015; Xu et al., 2019; Yang et al., 2019). Mutations in the catalytic SET domain of *Ezh2* have been identified from a variety of cancers; we created cell lines containing one of the inactivating mutations for our experiments (Antonysamy et al., 2013). We found that this mutation had a strong impact on H3K27me3 levels, but not on H3K27me2 levels. When these cells were differentiated in an undirected fashion they did not show the significant visual phenotypes seen with *Ezh2* knockout cells. While expression of some genes was altered, there were a number of PRC2 target genes that did not rely upon H3K27me3 for their regulation. The most dramatic phenotype observed was when cells were challenged to maintain their differentiated identity. Inhibitor treated and point mutated cells reverted readily to an ES phenotype when placed back into conditions that support ES cell growth. Thus, H3K27me3 was required for cells to maintain their identity rather than for the initial differentiation.

Results

PRC2 catalyzes di- and tri-methylation of histone H3 and is associated with gene repression. Previous studies have shown that deletion of PRC2 components in mouse ES cells has minimal effects on the undifferentiated, self-renewing state (Juan et al., 2016; Lavarone et al., 2019; Shen et al., 2008; Wassef et al., 2019). Yet deletion of EZH2, the catalytic subunit of PRC2, results in cells that do not differentiate and embryos that are reabsorbed by day E10.5 (Pasini et al., 2004). However, the requirements for specific methylation functions of PRC2 in differentiation and in the accompanying changes in gene expression have not been explored in detail. We examined the role for H3K27me3 in regulation by looking at stochastic differentiation of ES cells into embryoid bodies. Embryoid body (EB) formation is a well-studied method of undirected differentiation with predictable changes in gene expression (Fig 1A and (Behringer et al., 2016; Dang et al., 2002). Cells where PRC2 core components haven been deleted fail to form normal embryoid bodies, presumably because the cells apoptose when pushed to differentiate. Since PRC2 has been shown to play regulatory roles independent of H3K27 methylation, the exact requirement for the H3K27me3 modification at individual genes during differentiation as well as its role in maintaining cell identity remains unclear (Ahmed et al., 2018; Ai et al., 2017; Pereira et al., 2010).

127
128 **Inhibiting methyltransferase activity with the small molecule GSK343 does not block**
129 **differentiation potential**
130
131 As a starting point to understand the role of H3K27 methylation by PRC2 during ES cell
132 differentiation, we treated cells with the small molecule inhibitor GSK343 which blocks the
133 methyltransferase activity of EZH2 (Fioravanti et al., 2018; Lue & Amengual, 2018; Yang et al.,
134 2019). Treatment with DMSO was used as a control (Fig 1B). Unlike PRC2 knockouts, GSK343
135 treated cells form embryoid bodies that have a similar morphology to their DMSO treated
136 counterparts (Fig 1C.) Embryoid bodies formed after either DMSO or GSK343 treatment are
137 phenotypically similar to those made by WT cells. In contrast, PRC2 knockout cells tested in
138 parallel failed to form embryoid bodies ((Lavarone et al., 2019) and Fig. 2E). Thus, the inhibition
139 of methyltransferase activity can be phenotypically separated from PRC2 knockout cells.
140
141 To determine the molecular effects of blocking methyltransferase activity, we
142 performed RNA-seq experiments to compare changes in gene expression between cells treated
143 with the inhibitor and control over the differentiation time course. We examined PRC2 target
144 genes and found examples of genes whose expression pattern across differentiation was the
145 same in DMSO and GSK343 treated cells (e.g. Tbx3 or Sox3, Fig. 1D) as well as genes whose
146 expression was altered in GSK343 treated cells (e.g., Wnt3 and Itgb7, Fig 1D). The trends
147 observed with these two classes of genes were found to be mirrored in large sets of genes. We
148 classified PRC2 target genes into two sets, those that required H3K27me3 for their regulation
149 and those that do not need this modification to preserve normal gene expression patterns
150 during embryoid body formation. Genes were defined as independent of the H3K27me3
151 modification if their expression remained within 1.2 fold of the WT expression at all time points
152 (Fig 1E). We conclude that inhibiting methylation activity of PRC2 does not block differentiation
153 but does alter gene expression at a subset of genes though not at others.
154
155 **Point mutation to the SET domain inhibits methyltransferase activity**
156
157 We sought to extend and refine the findings made using GSK343 by generating a
158 hypomorphic mutation in *Ezh2* that had a defined impact on H3K27 methylation. We generated
159 mutant cells that allowed us to examine the contribution of H3K27 tri-methylation to gene
160 regulation and differentiation during EB formation. Inactivating point mutations in the SET
161 domain of EZH2 have been identified in several human cancers. We chose one of those
162 mutations, human R635C, which is analogous to mouse R681C, for analysis in mouse cells. This
163 residue is located in a region that is important for coordinating the methyl donor (Fig 2A and
164 (Antonysamy et al., 2013). We purified PRC2 complexes comprised of the core components
165 RBAP46/48, EED, SUZ12, EZH2 (WT or mutant) and the accessory protein AEBP2 (Supp. Fig. 2).
166 We confirmed that this residue is important for tri-methylation of H3K27 by PRC2 using an in
167 vitro methyltransferase assay. We compared it to WT EZH2 and another SET domain mutation
168 (722D) that has been previously shown to block methylation (Lavarone et al., 2019), Fig 2B).
169 The complexes that contained WT EZH2 methylated both core histones and purified H3 in a
170 time and concentration dependent manner (Supp. Fig. 2). In contrast, mutant complexes show

171 drastically reduced levels of activity. Using two separate purifications, residual activity of the
172 mutant complex was always under 2% of the purified WT complexes (Fig. 2B and Supp. Fig. 2).
173 We conclude that the *Ezh2* 681C mutation reduces the methyltransferase activity of the
174 complex by at least 50-fold.
175
176 We introduced the R681C mutation into the CJ7 mouse ES cell line using the CRISPR-
177 Cas9 system. We isolated two independent clones in the mouse ES cells line CJ7 with this
178 homozygous point mutation in the endogenous *Ezh2* gene (called CJ7 Ezh2$^{681C-99}$ and CJ7
179 Ezh2$^{681C-102}$). The phenotypes that we describe below were consistent between these two
180 independent lines. The mutant cells look phenotypically similar to WT cells and self-renew (Fig
181 2C). This was the anticipated result since knockout cells in the PRC2 core components EZH2 and
182 EED are also phenotypically similar to WT cells and can self-renew. We examined whether the
183 point mutation would lead to significant reduction of H3K27me3 in cells as anticipated from the
184 enzymatic defect seen in vitro. Lysine residues can be mono, di or tri-methylated. Mono-
185 methylation is spread broadly throughout the genome and di-methylation is loosely linked with
186 repressed genes, though this is poorly defined in most cell types. Tri-methylation of H3K27 is
187 closely associated with repressed genes, presumably due to binding of the CBX family of
188 proteins contained in the PRC1 complex to K27me3 and subsequent repression by this family of
189 complexes (Bernstein et al., 2006). We performed western blots on whole cell lysates from WT,
190 knockout and the point mutant cells and probed them with antibodies to di- and tri- H3K27
191 methylation and EZH2 (Fig 2D and Supp. Fig. 3). H3K27me3 was reduced to levels we could not
192 detect in the mutant cells, as was seen the knockout cells, but the levels of di-methylation were
193 largely unaffected in the R681C mutant cells. We conclude that in these cells the major effect of
194 the point mutation was to reduce the tri-methylation of H3K27. This is similar to the results
195 found in other studies of *Ezh2* point mutations (Lavarone et al., 2019). The R681C mutation
196 therefore offers an opportunity to examine the contribution of tri-methylated H3K27 to gene
197 regulation during differentiation.
198
199 We examined whether the mutant cell lines would form embryoid bodies similar to
200 those formed by WT cells, would apoptose like *Ezh2* or *Eed* knockout cells, or would take an
201 alternate path. We formed embryoid bodies by the hanging drop procedure and compared the
202 resultant phenotypes of WT, the point mutant and knockout cells. We found that the mutant
203 cells formed embryoid bodies, making them phenotypically separate from the knockout cells
204 (Fig 2E). This revealed that the dramatic reduction in H3K27me3 we see in the point mutant
205 cells does not stop the cells from differentiating, at least at a gross level. Another method for
206 testing the developmental potential of embryonic stem cells is assessing the formation of
207 beating clusters of cardiac cells. For this assay cells are differentiated in hanging drops and then
208 plated in individual wells to form a monolayer in differentiation media. After 10-15 days of
209 differentiation each well is visually examined for the presence of pulsing cells. Beating clusters
210 formed from both WT and mutant cells. There was some variation in the proportion of EBs that
211 could form beating clusters between the two 681C mutant strains, but in all cases the mutant
212 cells could form beating clusters (Fig. 2F). These data bolster the conclusion that the reduction
213 in H3K27me3 does not prevent cells from differentiating. This phenotype raised the issue of
214 whether there are molecular changes caused by the point mutation.

215
216 **Molecular phenotype of *Ezh2* point mutant cells**
217
218 To determine whether there were molecular phenotypes associated with the
219 hypomorphic mutation of *Ezh2*, and the resultant loss of H3K27me3, we determined the target
220 genes of PRC2 in our cell lines and measured their gene expression levels. We performed
221 CUT&RUN analysis using antibodies to H3K27me3, H3K27Ac, RING1b, EZH2 and SUZ12 in WT
222 and point mutant cells as embryonic stem cells (ESC) and as Embryoid bodies after
223 differentiation for eight days (D8EB). There have only been a small number of studies of PRC2
224 localization in differentiating cells, but of the approximately seven thousand target genes we
225 identified as having an H3K27me3 peak within 1kb of their transcription start site in WT cells,
226 just over 70% overlapped with previously published data (Fig. 3A and (Juan et al., 2016)). We
227 note that peaks called from our data set that did not overlap with previous called peaks showed
228 signal in the published data that was below the threshold, indicating further agreement
229 between the analysis done here and previous work. There were far more targets called using
230 the H3K27me3 than with the individual components of either polycomb complex, though the
231 targets are largely overlapping (Fig. 3B). This is likely due to differences in the strength of
232 individual antibodies. Therefore, we used the targets identified with H3K27me3 for further
233 analysis. In keeping with the western blot from whole cell lysates, H3K27me3 was reduced on
234 target genes in mutant cells (Fig. 3C). Levels of H3K27me3 were significantly lower in mutant
235 cells at day 4 of differentiation and then were increased at day 8 of differentiation but to levels
236 well below WT levels. The residual tri-methylation at day 8 might be due to EZH1 function
237 (Lavarone et al., 2019; Margueron et al., 2008; Shen et al., 2008). We focus below on the events
238 that happen during these first four days of differentiation and the impact of the lack of
239 H3K27me3 during this time frame. We conclude that the ability of the mutant cells to
240 differentiate was not due to retention of normal tri-methylation levels specifically on target
241 genes.
242
243 The experiments described above using small molecule inhibitors revealed that there
244 are genes that require H3K27me3 for their regulation and those that do not require H3K27me3
245 to maintain proper regulation. We investigated whether the point mutant cells showed these
246 same two gene classes. We performed RNA-seq analysis from ES cells and both D4 and D8EBs
247 from WT, CJ7 Ezh2$^{681C-99}$ and CJ7 Ezh2$^{681C-102}$ cells. The data for both mutant cell lines are nearly
248 overlapping and so for clarity we present the data from the CJ7 Ezh2$^{681C-99}$ (Supp. Fig. 4). For
249 this analysis we defined PRC2 target genes as those that had a statistically significant peak of
250 H3K27me3 from CUT&RUN at any time point in the EB formation protocol. PRC2 target genes
251 were identified using wild-type H3K27me3 peaks called by Homer using a p-value threshold of
252 0.001, a length of at least 1500 bp, 1rpkm in at least two time points and signal overlapping
253 Refseq annotated genes (TSS+-5kb). As with the cells treated with the small molecule inhibitor,
254 we could separate genes that rely on H3K27me3 from those that do not need a high level of the
255 modification for their regulation (Fig 3D). The gene expression patterns from the mutant cells
256 and the GSK343 treated cells clustered based upon day of differentiation rather than by
257 whether they were drug treated or mutant (Supp. Fig. 5), although the correlation was not as
258 strong as that seen between the two mutant cell lines. We detected both activated and

259 repressed genes that fell into methyltransferase-dependent and –independent categories. The
260 350 genes that are normally repressed during differentiation in WT cells, and were either
261 similarly repressed or were not repressed in mutant cells, showed more consistent patterns
262 than the genes that were normally activated in WT cells. These patterns were well established
263 by D4 of differentiation, thus we used repressed genes to further analyze any characteristics
264 specific to the methyltransferase dependent or to the independent genes.
265
266 We examined whether the level of H3K27me3 normally found on the genes in WT cells
267 or the amount of signal remaining in the mutant cells could predict whether a gene would be
268 dependent on the modification for its regulation. However, there was not a difference in the
269 levels of tri-methylation based on whether the genes require this modification for their
270 regulation (Fig. 3E). We then examined several characteristics of 350 genes that are normally
271 repressed during differentiation of WT ES cells including other histone modifications, CpG
272 methylation, and further sub dividing genes by their dependence on H3K27me3 (Supp. Fig. 6).
273 None of these characteristics showed any significant differences between genes who repression
274 was dependent upon methyltransferase activity and genes whose repression was not
275 dependent on methyltransferase activity. We conclude that there is a variable reliance on
276 H3K27me3 for gene regulation and that H3K27me3 is not the only driver of PRC2 target gene
277 repression during EB formation, just as full levels are not needed for differentiation.
278
279 **Methyltransferase point mutants cannot maintain differentiated cell identity**
280
281 A major issue in developmental gene expression concerns the interplay between
282 establishment and maintenance of gene expression profiles during differentiation. The
283 Polycomb group (PcG) system, including PRC2, plays a role in both aspects of gene regulation in
284 flies and in mammals. Substantial early work on mutant Drosophila highlighted a role for the
285 PcG, including gene products now known to compose PRC2, in maintenance. Given that we saw
286 limited impact of the ablation of H3K27me3 on establishment of the differentiated EB
287 phenotype, we tested whether the mutant or drug treated mouse cells were able to maintain a
288 differentiated state.
289
290 Under normal conditions, cells differentiated into embryoid bodies cannot revert to
291 ESCs without major manipulation such as introducing Yamanaka transcription factors
292 (Nakagawa et al., 2008; Takahashi & Yamanaka, 2006). To determine if the 681C point mutant
293 cells stably committed to a differentiated state, we formed day 8 EBs with WT and mutant cells,
294 dissociated the embryoid bodies into single cells and re-plated them in ESC conditions without
295 any additional manipulation. The cells were cultured in the ESC media for five days and then
296 stained for alkaline phosphatase (AP) activity. After incubation with an appropriate
297 colorometric substrate, ESCs become bright pink due to their alkaline phosphatase activity,
298 while feeder cells or any other differentiated cells remain unstained. We found a ten-fold
299 increase in the number of AP-positive colonies generated by the mutant cells over the WT (Fig.
300 4A and 4B). We asked whether this lack of commitment was maintained after longer periods of
301 differentiation and found that after 14 days there remained more cells that could revert to ES
302 cells, but to a considerably lesser extent than seen after 8 days (Figs. 4A, 4B). We conclude that

303 the mutant cells are not stably committed to the more defined lineages but can switch back to
304 an undifferentiated state, but that this flexibility decreases after two weeks of differentiation.
305
306 We used the small molecule inhibitor GSK343 to examine the time period during which
307 this flexibility is established. There were three possibilities: a) full levels of H3K27me3 might be
308 needed continuously to maintain the differentiated state; b) they might be needed at specific
309 times as the cells are differentiating; c) they might be needed only when cells are challenged
310 with external stimuli that allow reversion to embryonic stem cells. Examination of the mutant
311 cells addressed blocking full levels of methylation throughout the experimental time course,
312 but did not address the time period when that lack of activity was most important. To separate
313 the possibilities, we added or removed GSK343 during the differentiation time-course (Fig. 5A
314 shows the experimental design). To mimic the WT and point mutant conditions a subset of cells
315 were treated continuously with DMSO or GSK343 respectively. These treatments served as both
316 a baseline for altered times of GSK343 application. They also served to validate that the results
317 observed with re-plating of mutant cells were not caused by off target effects of the CRISPR
318 genetic manipulation or by mutations acquired during selection of these cells. Cells
319 continuously treated with GSK343 had higher numbers of AP-positive cells following re-plating
320 at 8 days, similar to the mutant cells; in contrast to the mutant cells there even more AP-
321 positive cells following re-plating after 14 days of differentiation in GSK343. GSK343 treatment
322 affects both di- and tri-methylation which might account for the increased plasticity seen at
323 later time points in drug treated cells (Supp. Fig. 7).
324
325 In addition to continual treatment with inhibitor, we varied the timing of GSK343
326 addition as depicted in Fig. 5A. Briefly, we treated ES cells for three days with either DMSO or
327 GSK343 before starting the differentiation. When embryoid body formation was initiated or at
328 day 4 of differentiation we changed the treatment from DMSO to GSK343 (or vice versa) for
329 half of the cells. We also switched the treatment at the time of re-plating into the ES conditions
330 at day 8. Finally, we allowed cells to differentiate to day 14 and switched treatment regimen
331 (Fig. 5A). The treatment type was switched just once in each scheme so we could determine
332 whether blocking the methylation of H3K27 at early or later stages of differentiation had the
333 greatest effect. These experiments allow us to determine whether reducing H3K27me3 has the
334 greatest effect on cell identity when the cells are differentiating, when they are challenged by
335 re-plating or throughout the differentiating time-course.
336
337 We found that the crucial window for treatment with the inhibitor was in the first four
338 days of embryoid body formation (Fig. 5A, B, C). Increased staining by alkaline phosphatase
339 activity was seen in all cells that had initially been treated with inhibitor, regardless of when it
340 was removed (Fig. 5C). Notably, treating with GSK343 for three days prior to inducing
341 differentiation, then removing the inhibitor when differentiation was initiated, led to a
342 significant increase in ES cells following re-plating at day 8. The only case where we saw
343 increased staining in re-plated cells that were initially treated with DMSO was when the
344 inhibitor was added at the onset of differentiation (Fig 5B, C). We conclude that the inhibition
345 of methyltransferase activity either immediately prior to differentiation or during the first four

346 days of differentiation allows the cells to remain in a more plastic state such that they can
347 revert to a stem cell-like phenotype when placed in the proper growth conditions.
348
349 When we examined the ability of treated cells to form beating colonies after treatment
350 with the small molecule we found no difference in the proportion of colonies that
351 spontaneously start beating between any of the treatment groups (Fig. 5D). This is consistent
352 with the data from the point mutant cells where both WT and mutant cells could form beating
353 colonies and further indicates that there is no deficit in the ability of the cells to differentiate
354 when H3K27 methylation is inhibited. Thus, as was seen with the comparison of WT and point
355 mutant cells, the obvious difference between DMSO and small molecule treated cells occurred
356 when cells were challenged to grow in the ESC culture conditions (Figs 5B,C). We conclude that
357 H3K27me3 methylation is more important in maintaining the differentiated state than in
358 generating that state, and that the critical time window occurs early in the differentiation
359 process.
360
361 The GSK343 treated cells and the mutant cells both appeared to revert to a pluripotent
362 state. To verify that these cells retained developmental potential we re-differentiated these
363 cells and determined whether they display the characteristic ability of ES cells to develop more
364 committed cells. We used the re-plated cells from both 681C mutant cells and those treated
365 with the inhibitor and attempted to make embryoid bodies. Both sets of re-plated cells were
366 able to make embryoid bodies, which confirms that they have developmental potential (Data
367 not shown).
368
369 To examine whether the reversion to a pluripotent state involved substantive changes in
370 gene expression, as opposed to gene expression changes in a few key genes, we examined
371 genome-wide gene expression pattern of the reverted cells and compared those to ESCs. To
372 examine the molecular phenotype of the re-plated cells, we isolated and sequenced RNA from
373 drug treated day 14 cells that were re-plated and had reverted to ES cell phenotype.
374 Unsupervised clustering showed that the average expression profiles of the cells that had been
375 treated with GSK343, and therefore had much higher levels of reversion, were more like WT ES
376 cells than to the DMSO treated and re-plated control cells (Fig. 5E.) We conclude that the cells
377 we see staining with alkaline phosphatase in our re-plating assays are reverting to an ES
378 phenotype. We examined the subset of PRC2 target genes that are normally repressed during
379 differentiation and found that many are reactivated when cells treated with GSK343 are re-
380 plated. This differs from the genes that are reactivated in the cells initially treated with DMSO.
381 The changes in gene expression observed following re-plating of cells treated with GSK343 were
382 significantly different from the patterns observed after re-plating of cells treated with DMSO.
383 (Supp. Fig. 7C). These expression pattern changes show the same response to the time of
384 treatment with GSK343 as seen above; reversion to the WT pattern requires GSK343 treatment
385 early in differentiation. From these data, we conclude that though all cells are placed under
386 developmental stress when re-plated into ES conditions, only those where H3K27 methylation
387 has been blocked revert to an ES cell phenotype. This underlines the importance of K3K27me3
388 in establishing the heritable gene expression profile of differentiated lineages.
389

390 **Discussion**
391
392 These studies offer two advances in understanding the role for tri-methylation of H3K27
393 during differentiation of ES cells into embryoid bodies. First, many PRC2 targets continue to be
394 regulated in a normal manner during the first four days of differentiation despite significantly
395 reduced H3K27me3 levels on these targets (Fig. 3.) Thus, H3K27me3 is not necessary for
396 repression of a significant set of PRC2 targets, indicating compensating mechanisms for
397 repression of these genes. Second, while many PRC2 targets are dysregulated when H3K27me3
398 is blocked, we did not observe a significant impact on differentiation. In contrast, there was a
399 large enhancement of the ability of differentiated cells to revert to a pluripotent phenotype
400 when placed into embryonic stem cell culture conditions. We conclude that the primary role for
401 H3K27me3 during early differentiation is maintenance of the differentiated state.
402
403 Differentiated WT cells are not generally capable of reverting to an ES phenotype when
404 their growth conditions are altered by a change in media. In normal cases, it takes the
405 reactivation of key transcription factors to allow cells to return to that state. In contrast, *Ezh2*
406 point mutant cells and those that that have been treated with a small molecule inhibitor readily
407 revert to an ES phenotype when placed into media that supports that type of growth. This was
408 seen at both the cellular and molecular level. When we varied the time windows where
409 inhibitor was present, we found that the crucial window for normal H3K27me3 levels was
410 between the start of differentiation through the first four days of embryoid body formation.
411 Not having the ability to add the tri-methylation modification at those early stages of
412 differentiation sets the stage for the cells to be able to revert to an ES phenotype when
413 challenged, even if H3K27me3 is restored later during embryoid body formation. In the setting
414 of the early stages of ES differentiation into embryoid bodies, the H3K27me3 modification is
415 acting analogously to a stopper on a swinging door. When the modification is present the door
416 will only open one way and the cells cannot go backward, but removal of the modification
417 enables the door to swing both ways allowing cells to go back and forth between the
418 differentiated and pluripotent state in response to external signals.
419
420 There are potential implications for these data in terms of the use of small molecule
421 inhibitors in therapeutic situations. Multiple adult cell types have different requirements for
422 PRC2 during their differentiation. Most relevant to the inhibition of PRC2 is the development of
423 blood cells. PRC2 is required for the differentiation of blood stem cells and is the site of some of
424 the highest levels of PRC2 expression in healthy adult tissues. If the phenotypes that we have
425 observed during embryoid body formation occur in a similar manner in blood stem cells,
426 treating patients with the small molecule inhibitors might alter the stability of commitment of
427 healthy stem cells, raising the possibility of novel cancers arising from cells that cannot stably
428 differentiate. Indeed, at least one clinical trial was temporarily suspended because patients had
429 developed novel cancers (Fioravanti et al., 2018; Harris, 2018; Italiano et al., 2018). Determining
430 the effect of blocking H3K27me3 in other differentiating cell lineages might be important to
431 clinical intervention by expanding the knowledge of the potential side effects.
432

We note that it is difficult to completely eliminate H3K27 methylation with mutations (Lavarone et al., 2019), and that the mutation we generated in *Ezh2* specifically impacts H3K27me3, especially early in differentiation, but does not eliminate all methylation of H3K27. This is both a limitation and an advantage; the significant impact on H3K27me3 early in differentiation allowed us to show that loss of tri-methylation has a potent phenotype (unstable commitment) at this stage yet does not have a discernible differentiation phenotype. These data demonstrate a striking difference in the dependency of these two key phenotypes on H3K27me3. This *Ezh2* mutation also has a molecular phenotype when gene regulation is examined, raising the possibility that the network of genes that require H3K27me3 for appropriate regulation at this stage are primarily responsible for driving stable commitment to the differentiated state.

Methods

Cell Culture

ES cells: CJ7 WT, CJ7 *Ezh2*-/- and CJ7 *Eed*-/- cells were a generous gift from the laboratory of Stuart Orkin. We cultured all embryonic stem cells on a monolayer of feeder MEFs in ES media (DMEM (Gibco 11995-506) supplemented with 20%FBS, NEAA, pen/strep, glutamax, and LIF) on tissue culture treated flasks coated with 0.2% geletin. Media was changed daily and cells were split every 2-3 days.

EZH2 point mutant Cells: Point mutations were introduced into CJ7 WT using CRISPR RNP transfected into cells with the Amaxa mouse ES kit (Lonza VPH-1001). $1x10^6$ cells were transfected with the RNP containing two separate guide RNAs a single stranded donor oligo and a linearized puromycin resistance gene. Cells were plated into three wells of a six well plate with puroR MEFs and regular ES media. The next day puromycin was added to the wells in a range of concentrations and kept on the cells for the next two days. Following selection, resistant cells were expanded, individual colonies were then re-plated into twenty-four well plates and checked for the presence of the mutation by restriction enzyme digestion followed by confirmation with sequencing.

EB formation: Embryoid bodies were formed using the hanging drop method(Behringer et al., 2016; Dang et al., 2002). Briefly, ES cells were trypsinized, de-MEFed and then resuspended in differentiation media (IMDM (Gibco 12440-053) supplemented with 20% FBS, pen/strep, and glutamax. No LIF). Droplets containing approximately 180 cells were incubated for four days so that spheres of differentiating cells could form. After the four days EBs were collected and grown in suspension in non-adherent plates or used for subsequent experiments.

Beating heart assay: Beating clusters were differentiated from day 4 embryoid bodies (Boheler et al., 2002; Hescheler et al., 1997). Individual EBs were transferred into individual wells of a gelatinized 12 well plate. Cells were maintained in differentiation media throughout the experiment. Wells were monitored for beating colonies for the next 15 days and were scored as positive if there were any beating cells in that time period.

477 **Western Blot**
478 The antibodies that were used probe the Western blots were from Cell Signaling Technology
479 H3K27me3 (9733S) and H3K27me2 (9728S) as well as from EMD Millipore EZH2 (07-689).
480
481 **RNA-seq**
482 RNA was isolated from whole cells using the Nucleospin RNA kit from Macherey Nagel
483 (740955.50). We then depleted rRNA using the Ribozero Gold kit from Epicentre (RZG1224).
484 cDNA was synthesized from the purified RNA using the Superscript Vilo cDNA sequencing kit
485 from ThermoFisher (11754050) the libraries were assembled as previously described (Bowman
486 et al., 2013). Three replicates were completed for all experimental conditions except the Day 14
487 re-plated cells where two replicates were completed.
488
489 **Methyltransferase Assay**
490 Purified protein complexes were incubated at room temperature with a histone substrate at a
491 final concentration of 500nM and approximately 500nM radioactive SAM (Adenosyl-L-
492 methionine S-methyl^{3}H from PerkinElmer (NET155H250UC)) in methyltransferase buffer (10%
493 glycerol, 25mM HEPES PH 7.9, 2mM MgCl with 1mM DTT added fresh). Unless otherwise
494 specified all reactions ran for one hour before being stopped with the addition of 6x SDS buffer.
495 Samples were then run on an SDS page gel, coomassie stained and incubated in AMPLIFY
496 Amersham/GE (NAMP100) for 20 minutes. The gel was dried and exposed to film for a
497 minimum of 24 hours before developing.
498
499 **Protein purification**
500 The ORF for each member of the core PRC2 complex were cloned into the pFastBac1
501 baculovirus with Suz12 tagged with 3xFlag. Sf9 transfection with bacmid DNA and virus
502 amplification were performed essentially as described for the Bac-to-Bac Baculovirus
503 Expression System (ThermoFisher Scientific). Sf9 cells were maintained in Hyclone CCM3
504 (CCM3 liquid medium with L-glutamine, GE Healthcare Life Sciences SH30065.02)
505 supplemented with 50 U/ml Penicillin-Streptomycin (ThermoFisher Scientific, 15140-122). For
506 protein expression, $2x10^6$ Sf9 cells/ml were infected at an MOI of approximately 10. Cells were
507 harvested 66 hours post infection by centrifugation at 5000xG for 15 minutes. Cells were lysed,
508 treated with DNAse1 then the complex was bound to M2 and the complex was eluted with flag
509 peptide.
510
511 **CUT&RUN**
512 CUT&RUN experiments were performed as described (Skene & Henikoff, 2017). The antibodies
513 we used were from Cell Signaling Technology H3K27me3 (9733S), EZH2 (5246S), SUZ12 (3737S)
514 and Bethyl laboratories RING1b (A302-869A). Libraries were constructed as described in the
515 RNA-seq section. Two replicates were completed and representative experiments are shown.
516
517 **Alkaline Phosphotase Assay**
518 Cells were stained according to the instructions in the Stemgent AP Staining Kit II from
519 Reprocell (00-0055). Images of stained wells were quantified using ImageJ FIJI software.
520

521 **Bioinformatics Methods**
522
523 RNA-seq data processing: All RNA sequencing reads were aligned to the mm10 genome using
524 STAR v2.5.3 (Dobin et al., 2013). Gene annotations were obtained from Ensembl (Hunt et al.,
525 2018) Genome browser tracks were generated using Homer v4.10.3 (Heinz et al., 2010) and
526 visualized in IGV (Robinson et al., 2011). Reads in exons of Refseq annotated genes were
527 counted using featureCounts v1.6.1(Liao et al., 2014). edgeR (Robinson et al., 2010) was used to
528 normalize reads and calculate FDR using triplicates. All further calculations and figures were
529 made using R v3.3.2 (Dessau & Pipper, 2008). For all heatmaps, standard z-scores calculations
530 were made using average RPKMs of triplicates for each gene across all conditions. Genes were
531 narrowed down to only PRC2 targets using H3K27me3 CUT&RUN data. Only genes changing in
532 untreated or wild-type cells over the time-course were used for further analysis. The genes
533 were filtered using cut-offs of at least 0.5 RPKM average expression at any timepoint, at least
534 1.5 fold-change and maximum 0.05 FDR while comparing Day 8 and Day 4 or Day 4 and Day 0.
535 Genes were then clustered based on up or down-regulation in control cells and up or down-
536 regulation or unchanged gene expression in mutant or treated cells.
537
538 For Fig. 5E, unsupervised clustering was performed using R's heatmap.2 function. CpG and GC
539 levels were calculated using Homer's annotatePeaks function.
540
541 CUT&RUN data processing: All CUT&RUN reads were aligned to the mm10 genome using
542 bowtie2 and filtered using samtools (Li et al., 2009) to keep uniquely aligned reads. Genome
543 browser tracks were generated using Homer v4.10.3 and visualized in IGV. Peaks were called
544 using Homer's findPeaks function for broad peaks. PRC2 target genes were identified using
545 wild-type H3K27me3 peaks at least 1500 bp in length, 1rpkm in at least two time points and
546 overlapping Refseq annotated genes (TSS+-5kb). Deeptools v3.3.0(Ramírez et al., 2014) was
547 used to make average profile plots for Fig. 3E.
548
549 Published ChIP-seq data sources and processing: Published data for other canonical and non-
550 canonical PRC2 components was downloaded from GEO as follows : H3K27me3 (GSM2282188,
551 GSM2282191, GSM2282192) (Juan et al., 2016), EPOP (GSM2098943) (Beringer et al., 2016),
552 Jarid2 (GSM491760) (Li et al., 2010), H3K4me1 (GSM1180178), H3K4me3 (GSM1180179),
553 H3K9me3 (GSM1180180), H3K36me3 (GSM1180183) (Hon et al., 2014). FASTQ files were
554 downloaded from GEO using sratools v2.9.1 (https://ncbi.github.io/sra-tools/). All reads were
555 aligned to the mm10 genome using bowtie2 and filtered using samtools to keep uniquely
556 aligned reads. Genome browser tracks were generated using Homer v4.10.3. Deeptools v3.3.0
557 was used to make average profile plots for Fig. 3C and E.
558
559

Figure 1.

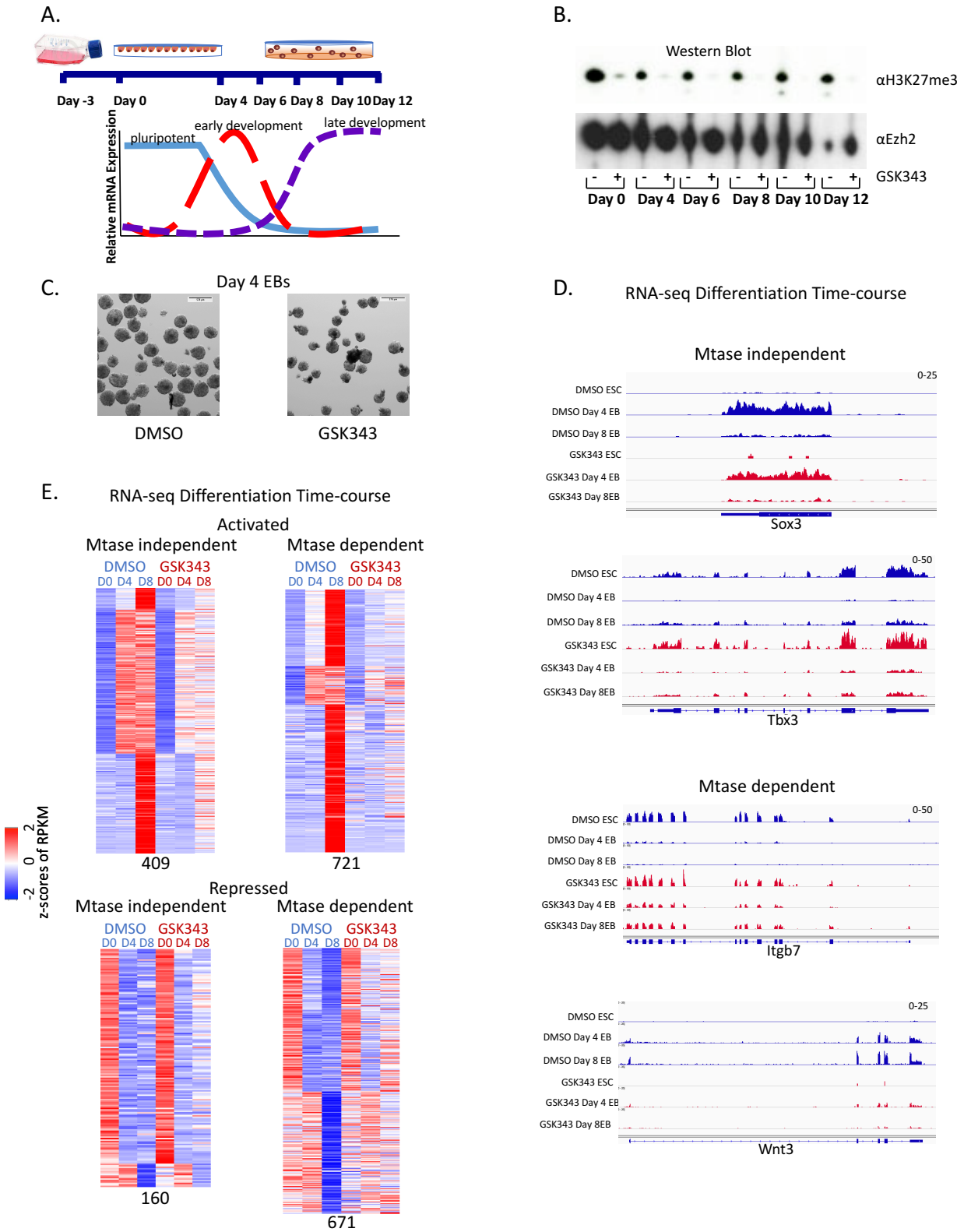
A.
Day -3
Day 0
Day 4
Day 6
Day 8
Day 10
Day 12
pluripotent
early development
late development
Relative mRNA Expression
B.
Western Blot
αH3K27me3
αEzh2
GSK343
Day 0
Day 4
Day 6
Day 8
Day 10
Day 12
C.
Day 4 EBs
DMSO
GSK343
D.
RNA-seq Differentiation Time-course
Mtase independent
DMSO ESC
DMSO Day 4 EB
DMSO Day 8 EB
GSK343 ESC
GSK343 Day 4 EB
GSK343 Day 8EB
Sox3
Tbx3
Mtase dependent
Itgb7
Wnt3
E.
RNA-seq Differentiation Time-course
Activated
Mtase independent
Mtase dependent
DMSO
GSK343
D0 D4 D8 D0 D4 D8
409
721
Repressed
160
671
z-scores of RPKM

560

Figure 2.

A.

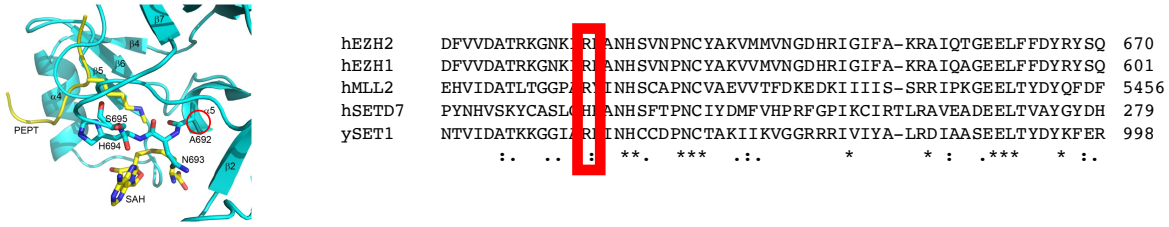

B.

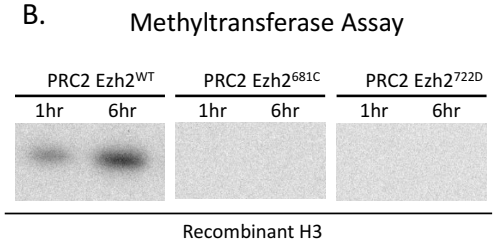

C.

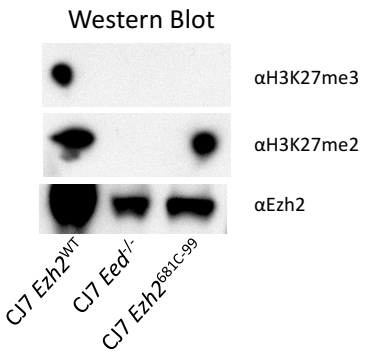

D.

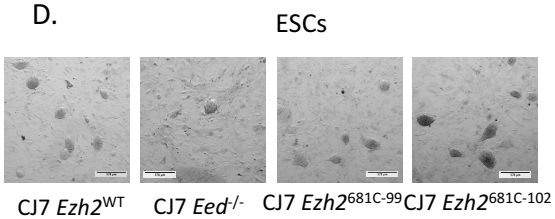

E.

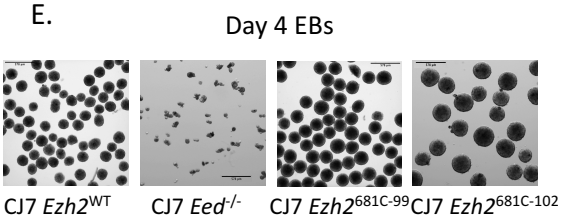

F.

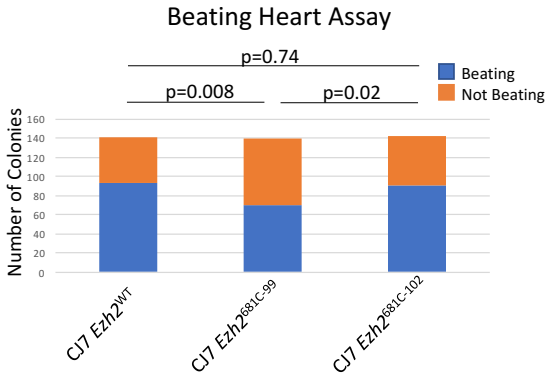

561
562

Figure 3.

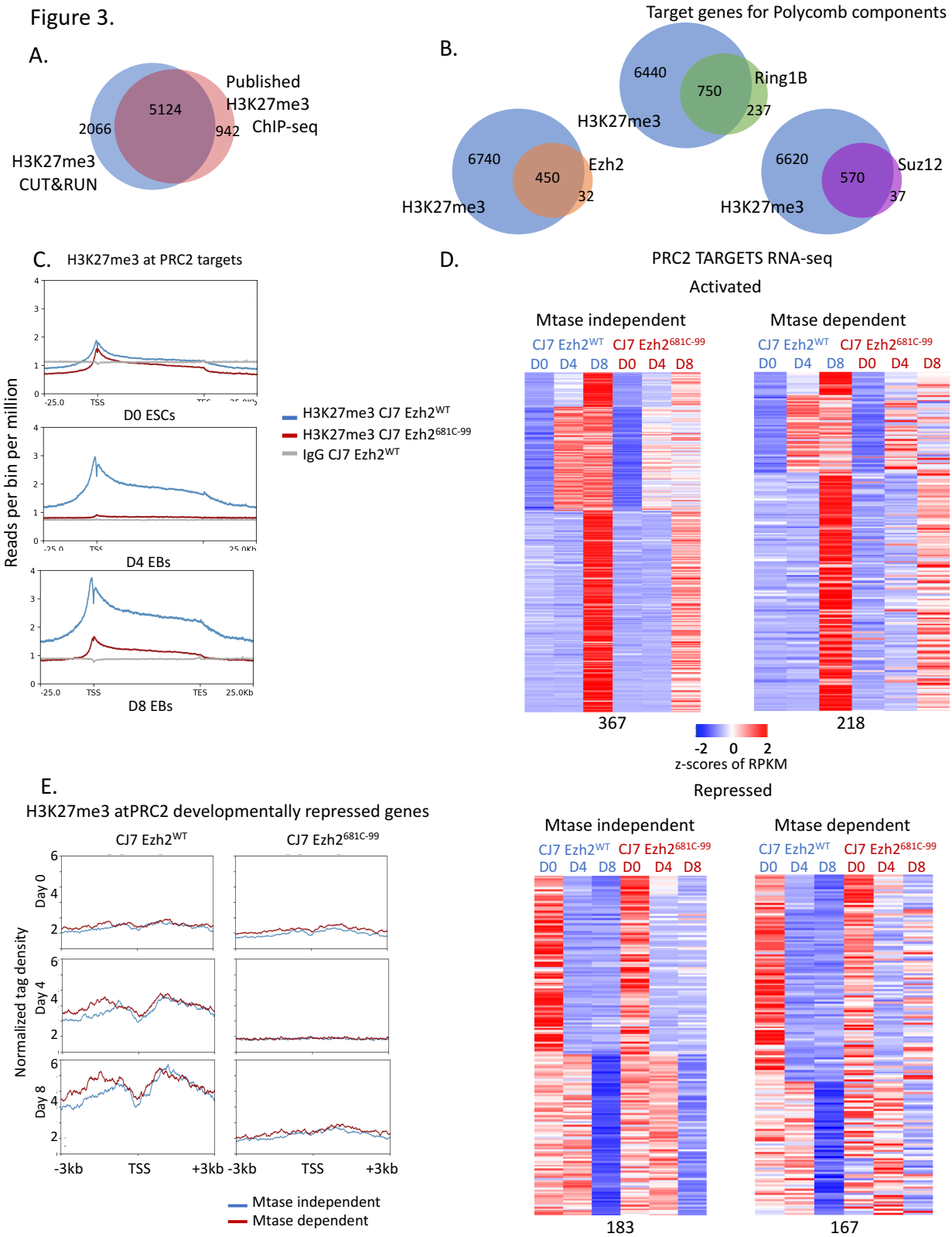
A.
Published H3K27me3 ChIP-seq
5124
2066
942
H3K27me3 CUT&RUN
B.
Target genes for Polycomb components
6440
750
Ring1B
237
H3K27me3
6740
450
Ezh2
32
H3K27me3
6620
570
Suz12
37
H3K27me3
C. H3K27me3 at PRC2 targets
Reads per bin per million
D0 ESCs
D4 EBs
D8 EBs
-25.0
TSS
TES
25.0Kb
H3K27me3 CJ7 Ezh2WT
H3K27me3 CJ7 Ezh2681C-99
IgG CJ7 Ezh2WT
D.
PRC2 TARGETS RNA-seq
Activated
Mtase independent
Mtase dependent
CJ7 Ezh2WT CJ7 Ezh2681C-99
D0 D4 D8 D0 D4 D8
367
218
-2 0 2
z-scores of RPKM
Repressed
183
167
E.
H3K27me3 atPRC2 developmentally repressed genes
CJ7 Ezh2WT
CJ7 Ezh2681C-99
Normalized tag density
Day 0
Day 4
Day 8
-3kb
TSS
+3kb
Mtase independent
Mtase dependent

563

Figure 4.

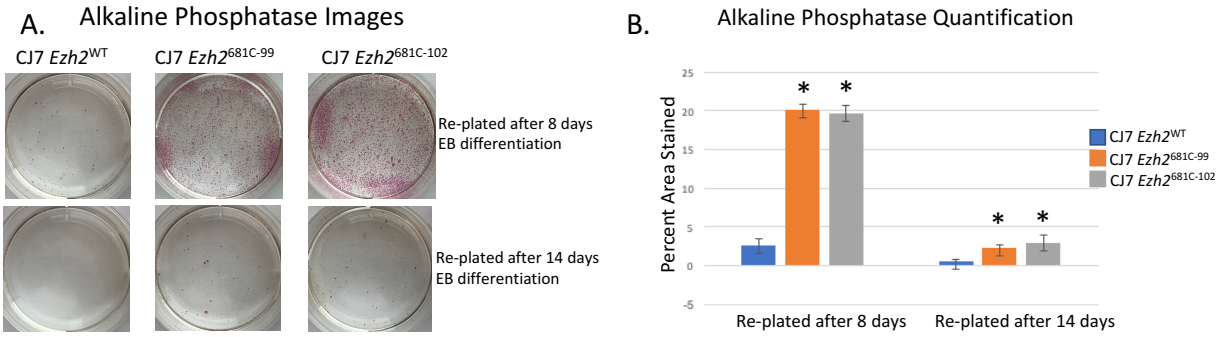

564
565

Figure 5.

A.

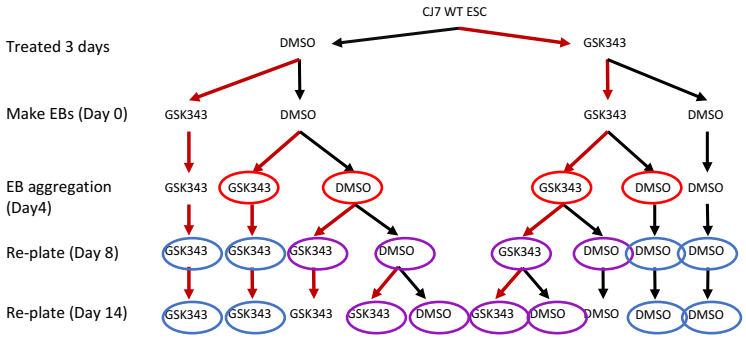

B.

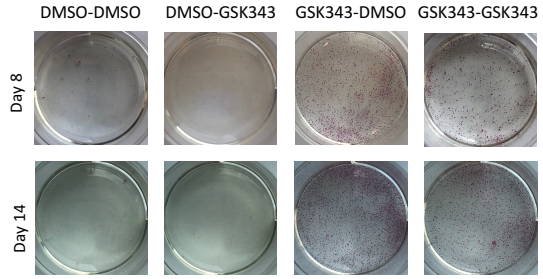

C.

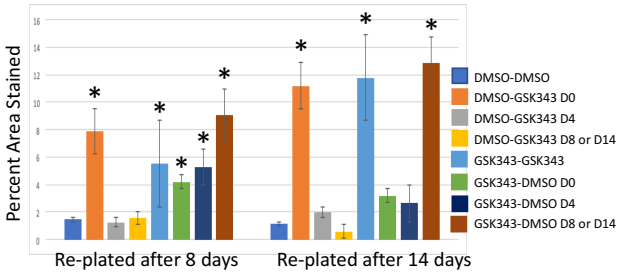

D.

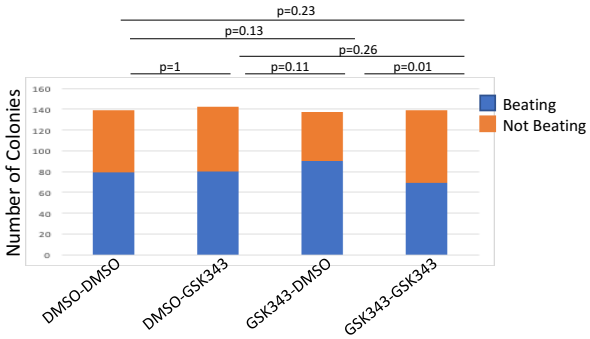

E.

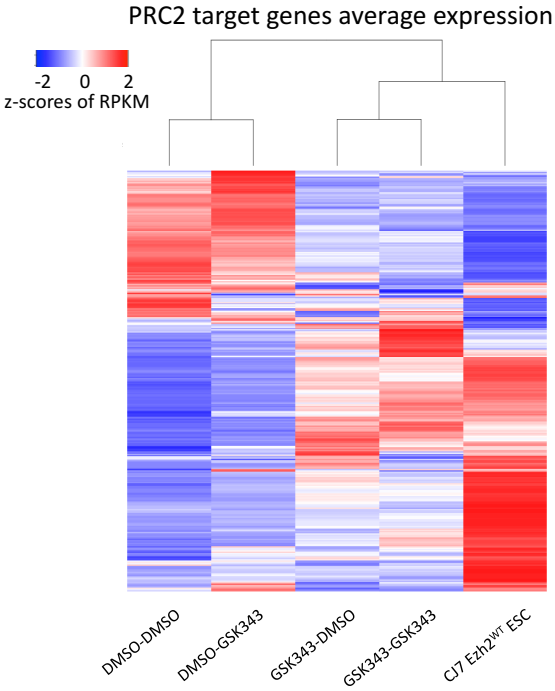

566
567

568 Figure Legends:
569
570 Figure 1
571 (A) Diagram of embryoid body (EB) formation time-course. (B) Western blot of cells treated
572 with GSK343 EZH2 inhibitor or DMSO control probed with H3K27me3 and EZH2 antibodies. (C)
573 54x magnification of day 4 EBs from cells treated with either DMSO control or GSK343. (D)
574 Screen shots from RNA-seq over the EB differentiation time-course from Mtase independent
575 (Sox3 and Tbx3) and Mtase dependent (Itgb7 and Wnt3) genes from cells treated with DMSO
576 (blue) or GSK343 (red). (E) Heatmap showing expression patterns of Mtase dependent and
577 independent genes in untreated (DMSO) and treated (GSK343) ES cells over development time-
578 course. Z-scores of average RPKMs of duplicates are shown for each gene across all samples.
579 Genes are separated based on if they were activated (top) or repressed (bottom) in untreated
580 cells over time as well as if they had a similar expression pattern in treated cells (Mtase
581 dependent genes) (left) or a different expression pattern (Mtase independent genes) (right).
582 The four groups are further clustered based on fold-changes over time in untreated cells.
583
584 Figure 2
585 (A) Diagram of *Ezh2* SET domain structure with the 681 residue circled and an alignment of SET
586 domains with the analogous residue highlighted in red adapted from (Antonysamy et al., 2013).
587 It is highly conserved across species and methyltransferases. (B) In vitro methyltransferase
588 assay with PRC2 comprised of WT or mutant EZH2, EED, SUZ12, and AEBP2. Recombinant H3 is
589 the substrate and a radioactive SAM was the methyl donor. Reactions progressed for 1 or 6
590 hours. (C) Western blot from WT, mutant and PRC2 knockout cells probed with H3K27me and
591 EZH2 antibodies. (D) 54x magnification of embryonic stem cells (ESCs) WT, 681C-99, 681C-102
592 and *Eed*$^{-/-}$ cells. (E) 54x magnification of embryoid bodies that have differentiated for 4 days
593 from WT, 681C-99, 681C-102 and *Eed*$^{-/-}$ cells. (F) Quantification of beating heart assay from WT,
594 681C-99 and 681C-102 cells that were differentiated as EBs for 4 days and then individually
595 plated in differentiation media. Blue shows the number of EBs that gave rise to beating cells
596 and Orange shows those that did not.
597
598
599
600 Figure 3
601 (A) Venn diagram showing overlap of H3K27me3 cut-and-run and published ChIP-seq data
602 peaks. (B) Venn diagrams showing overlap of target genes of H3K27me3 and other PRC2
603 components by cut-and-run. (C) Average profiles showing H3K27me3 cut-and-run versus IgG
604 control signal at Day0, 4 and 8 in wild-type and mutant cells. (D) Heatmap showing expression
605 patterns of Mtase dependent and independent genes in wild-type and mutant ES cells over
606 developmental time-course. Z-scores of average RPKMs of triplicates are shown for each gene
607 across all samples. Genes are separated based on if they were activated (left two panels) or
608 repressed (right two panels) in wild-type cells over time as well as if they had a similar
609 expression pattern in mutant cells (Mtase dependent genes) or a different expression pattern
610 (Mtase independent genes). The four groups are further clustered based on fold-changes over
611 time in untreated cells. (E) Average profiles showing H3K27me3 binding in wild-type and

612 mutant cells by cut-and-run at Mtase dependent or independent and developmentally
613 repressed PRC2 target genes over the time course.
614
615 Figure 4
616 (A) Alkaline phosphatase staining from WT, 681C-99 and 681C-102 cells that had been
617 differentiated for 8 or 14 days and then transferred into ESC conditions for five days before
618 staining. ESCs stain bright pink in this assay. (B) Quantification of alkaline phosphatase staining
619 from re-plated cells with standard deviation error bars. Samples with significant difference
620 ($p<0.05$) from WT cells marked with an asterisk.
621
622
623 Figure 5
624 (A) Diagram showing the drug treatment plan for differentiation and re-plating of cells. Red
625 circles indicate the cells used for the beating heart assay (D), Purple are shown in images in (B)
626 as well as quantified in (C) and blue circles highlight samples only quantified in (C). (B) Alkaline
627 phosphatase staining from treated cells re-plated after 8 or 14 days of EB differentiation. Only
628 cells that start in GSK343 treatment is stain pink indicating that the cells have reverted to an ES
629 phenotype. (C) Quantification of alkaline phosphatase staining from cells treated with DMSO or
630 GSK343. Time of the treatment switch is indicated in the legend. Samples with significant
631 differences from those continuously treated with DMSO ($p<0.05$) are marked with an asterisk.
632 (D) Quantification of beating heart assay with GSK343 and DMSO treated cells. Cells were
633 differentiated as EBs for 4 days and then plated into differentiation media. Blue indicates the
634 number of EBs that formed beating cells and orange indicates the number that did not. (E)
635 Unsupervised clustering of RNA-seq average expression of cells re-plated for 5 days after 14
636 days of EB formation. Cells that were treated with GSK343 have gene expression profiles that
637 cluster with average expression from WT ESCs.
638

Supp. Fig. 1

A.

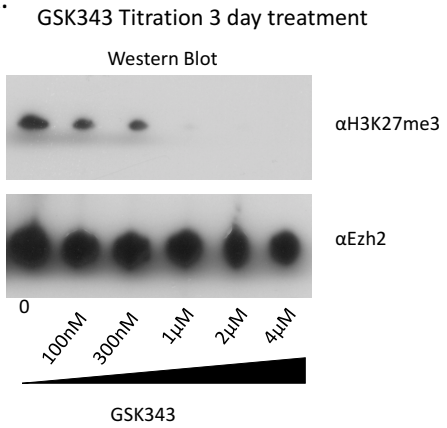

Supp. Fig. 2

A.

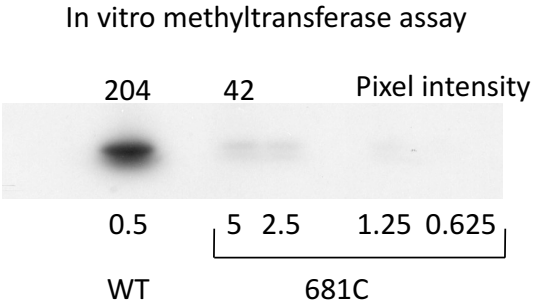

C.

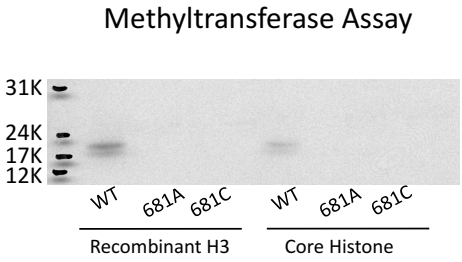

B.

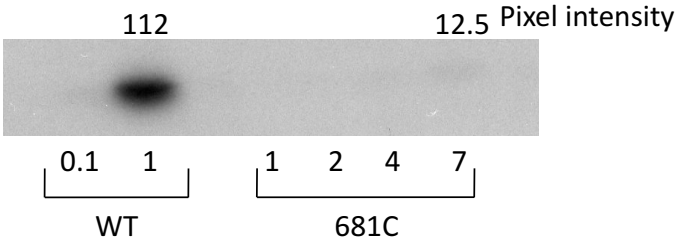

D.

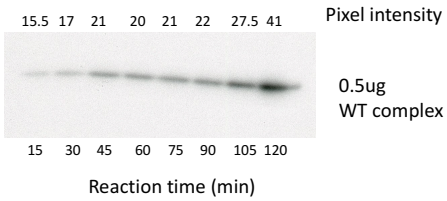

639

Supp. Fig. 3

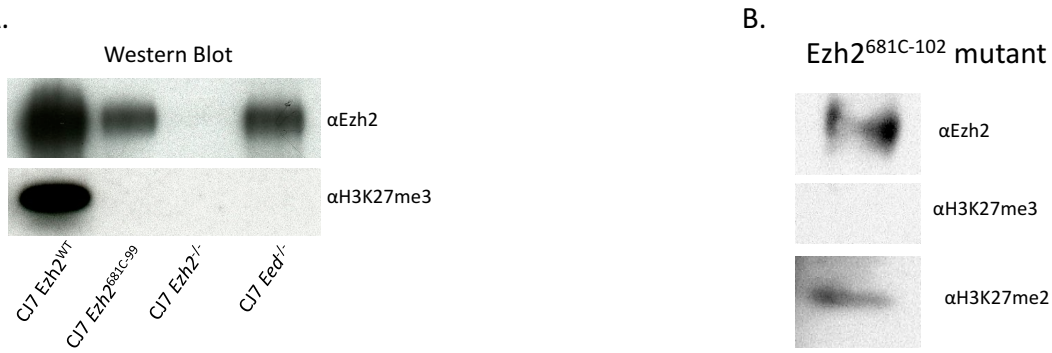

640

Supp. Fig. 4

A.

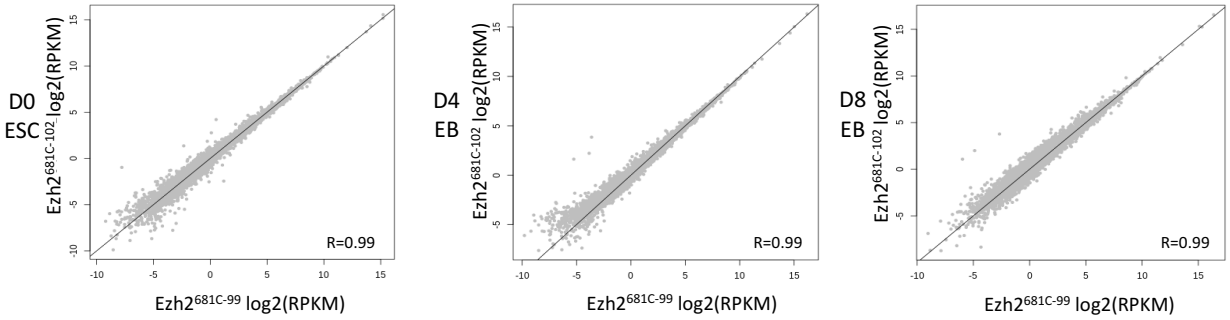

B.

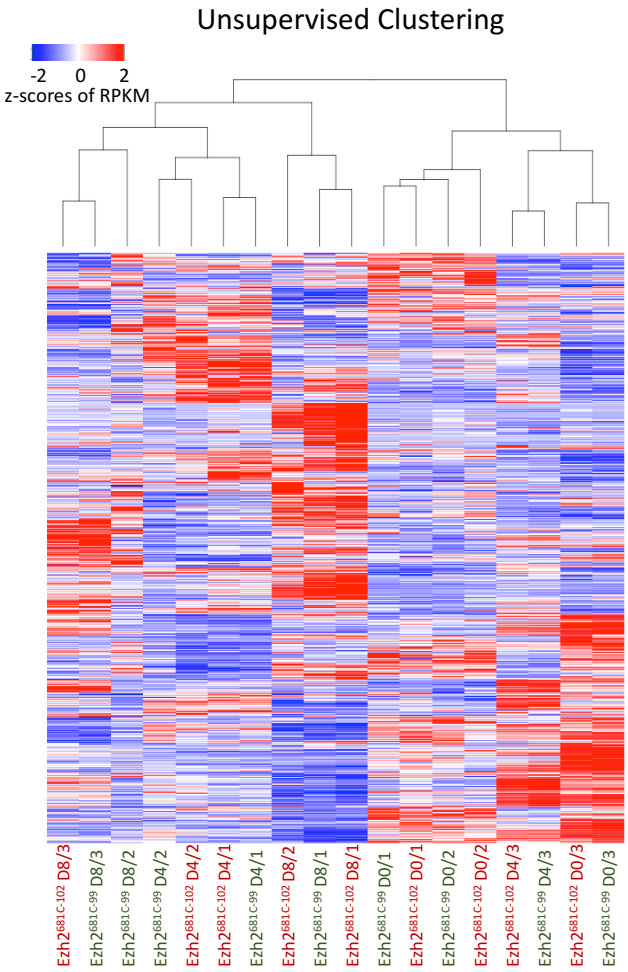

641

Supp. Fig. 5

Log2 fold-change as compared to WT comparisons between drug treated and mutant cells

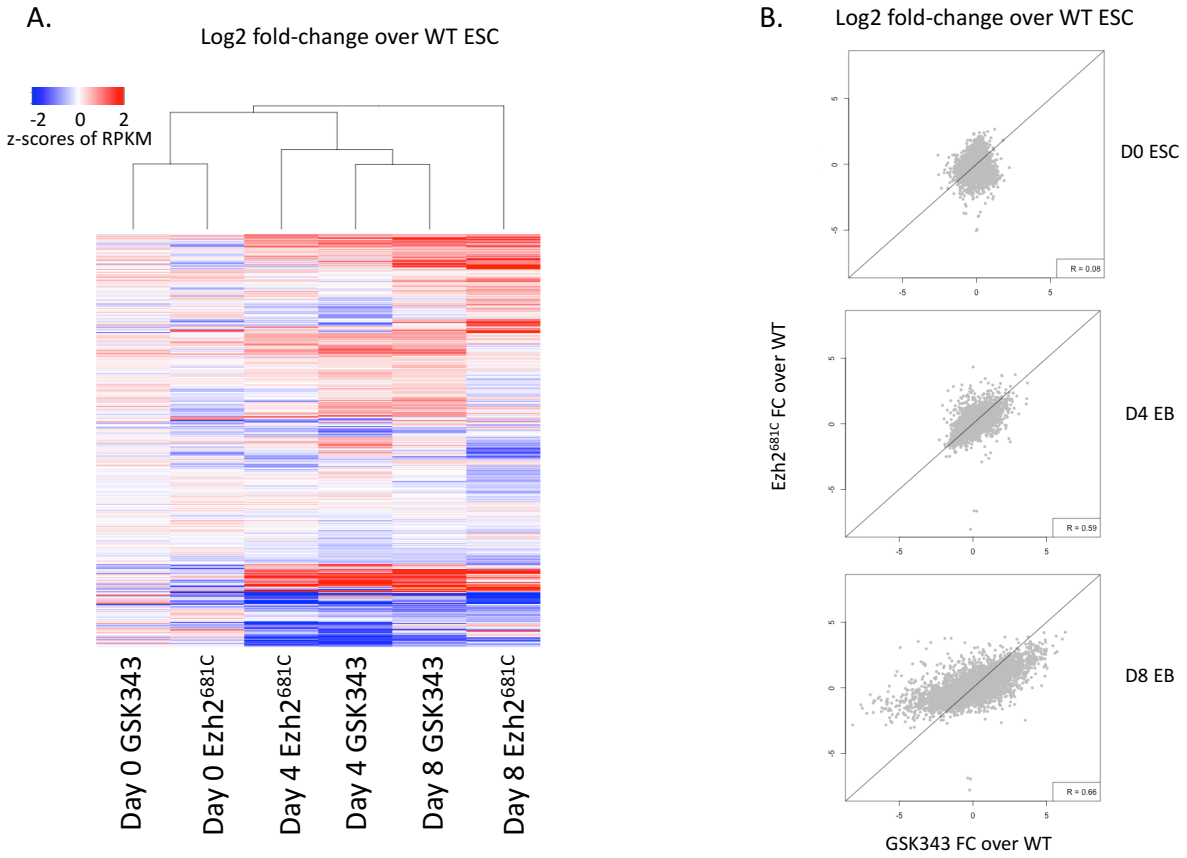

642

Supp. Fig. 6.

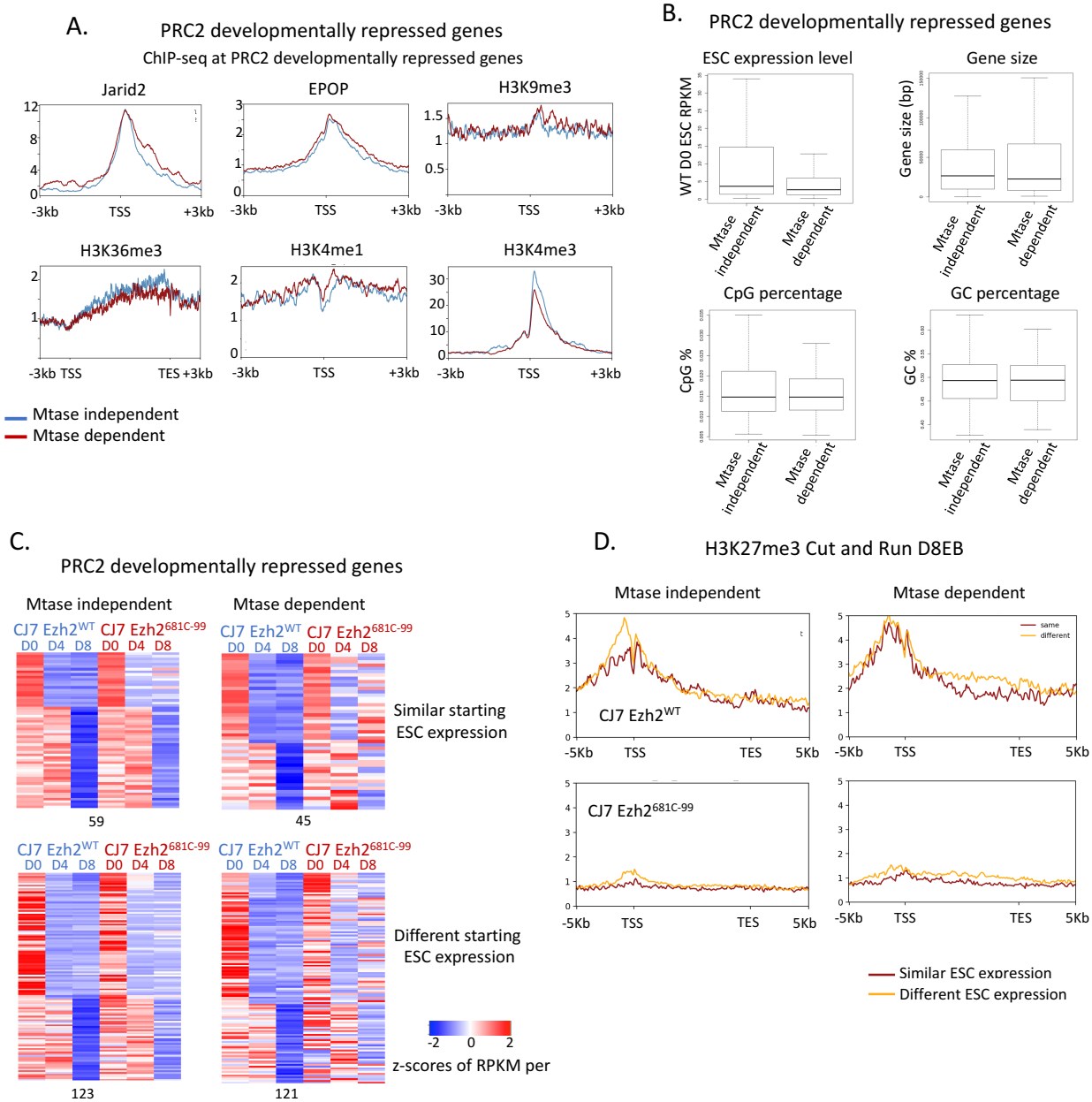

643

Supp. Fig. 7.

A.

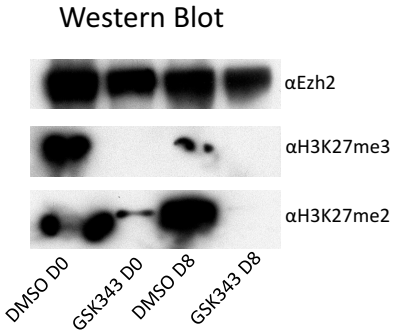

B.

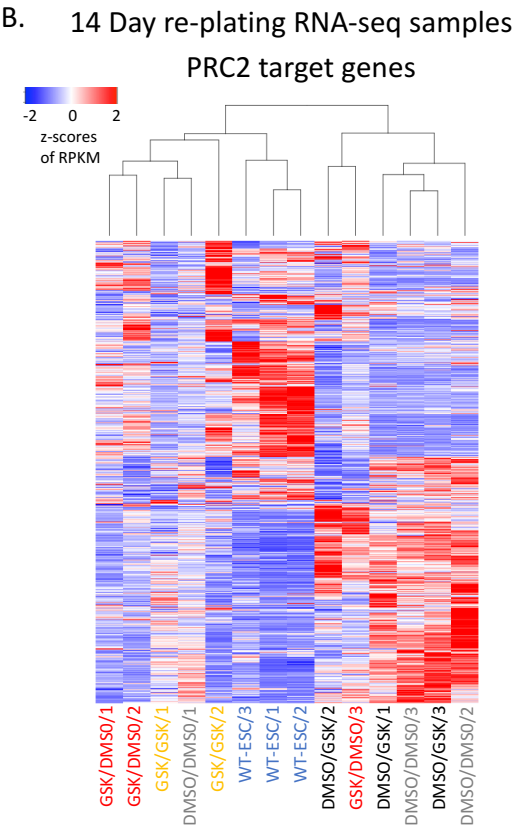

C.

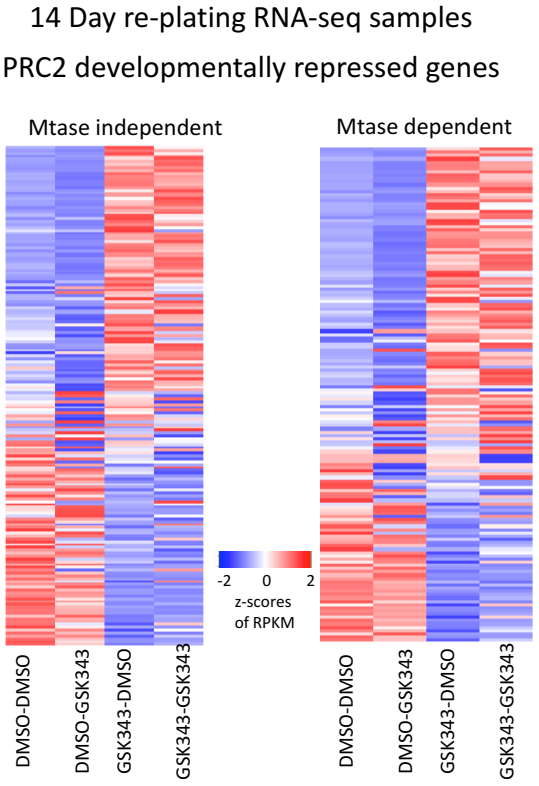

644
645

646 Supplemental Figure Legends
647
648 Supp. Fig. 1
649 (A) Western blot of WT CJ7 cells treated for three days with an increasing concentration of
650 GSK343 probed with antibodies to H3K27me3 and EZH2. The 4uM concentration was non-toxic
651 to cells and yielded a loss of H3K27me3 signal and so this concentration was used for all
652 experiments.
653
654 Supp. Fig. 2
655 (A,B) In vitro methyltransferase assay comparing EZH2-WT and EZH2-681C. Concentration of
656 the PRC2 complex is indicated below the image with pixel intensity indicated above. (C) In vitro
657 methyltransferase assay with WT, 681A and 681C complexes with both recombinant histones
658 that do not have any covalent modifications and core histones that do as the substrate. With
659 both substrates, the mutant complexes did not show signal. (D) In vitro methyltransferase assay
660 with WT complex over time. All other methyltransferase assays shown here were done for 60
661 minutes which is well within the linear range.
662
663 Supp. Fig. 3
664 (A) Western blot showing the EZH2 and H3K27me3 signal for WT, EZH2 mutant and PRC2 KO
665 cells. (B) Western blot showing the EZH2, H3K27me3 and H3K27me2 signal of $EZH2^{618C-102}$
666 mutant cells.
667
668 Supp. Fig. 4
669 (A) Comparisons between $Ezh2^{618C-99}$ and $Ezh2^{681C-102}$ RNA-seq over the differentiation time-
670 course. The two mutants are nearly identical at all time points. (B) Unsupervised clustering of
671 the mutant RNA-seq showing that the day of differentiation is more relevant predictor of
672 similarity rather than the mutant strain.
673
674 Supp. Fig. 5
675 (A) Unsupervised clustering showing the fold change over WT ESC of GSK343 treated or
676 Ezh2681C-99 cells. The day of differentiation is the stronger predictor of clustering. (B) Direct
677 comparison of mutant and drug treated cells RNA-seq fold change over WT gene expression.
678
679 Supp. Fig. 6
680 (A) Average profiles showing binding of other PRC2 components and histone marks in wild-type
681 and mutant cells at Mtase dependent or independent and developmentally repressed PRC2
682 target genes over the time course. (B) Boxplots showing comparisons of different
683 characteristics of Mtase dependent and independent, developmentally repressed PRC2 target
684 genes in wild-type and mutant cells. (C) Heatmaps showing developmentally repressed genes
685 from Fig 3(D), separated based on expression levels of wild-type and mutant ES cells at Day 0 of
686 the time-course. Genes with similar expression levels at Day 0 in wild-type and mutant (within
687 1.2 fold) are on the top and those with different starting expression levels (more than 1.2 fold)
688 are at the bottom. (D) Average profiles showing H3K27me3 binding in wild-type and mutant
689 cells by cut-and-run at Mtase dependent or independent and developmentally repressed PRC2

690 target genes that have either different (more than 1.2 fold) or similar (within 1.2 fold)
691 expression over the time course.
692
693 Supp. Fig. 7
694 (A) Western blot of CJ7 cells treated with DMSO or GSK343 showing the (levels of Ezh2,
695 H3K27me3 and H3K27me2 at Day 0 and Day 8 or EB formation. B) Unsupervised clustering of
696 PRC2 target genes in re-plated cells and wild-type ES-cells. Untreated or drug treated cells were
697 replated at 14 days in DMSO or GSK343. Z-scores of average RPKMs of triplicates (duplicates for
698 GSK-GSK) are shown for each gene across all samples. (C) Heatmaps showing comparison of
699 treated and untreated cells, re-plated in DMSO or GSK343 for previously identified Mtase
700 dependent and independent genes. Z-scores of average RPKMs of triplicates (duplicates for
701 GSK-GSK) are shown for each gene across all samples.
702
703
704
705 Abdel Raouf, S. M., Ibrahim, T. R., Abdelaziz, L. A., Farid, M. I., & Mohamed, S. Y. (2019, Dec 10).
706 Prognostic Value of TWIST1 and EZH2 Expression in Colon Cancer. *J Gastrointest Cancer*.
707 https://doi.org/10.1007/s12029-019-00344-4
708
709 Ahmed, A., Wang, T., & Delgado-Olguin, P. (2018). Ezh2 is not required for cardiac regeneration
710 in neonatal mice. *PLoS One, 13*(2), e0192238.
711 https://doi.org/10.1371/journal.pone.0192238
712
713 Ai, S., Peng, Y., Li, C., Gu, F., Yu, X., Yue, Y., Ma, Q., Chen, J., Lin, Z., Zhou, P., Xie, H., Prendiville,
714 T. W., Zheng, W., Liu, Y., Orkin, S. H., Wang, D. Z., Yu, J., Pu, W. T., & He, A. (2017, Apr
715 10). EED orchestration of heart maturation through interaction with HDACs is
716 H3K27me3-independent. *Elife, 6*. https://doi.org/10.7554/eLife.24570
717
718 Aloia, L., Di Stefano, B., & Di Croce, L. (2013, Jun). Polycomb complexes in stem cells and
719 embryonic development. *Development, 140*(12), 2525-2534.
720 https://doi.org/10.1242/dev.091553
721
722 Antonysamy, S., Condon, B., Druzina, Z., Bonanno, J. B., Gheyi, T., Zhang, F., MacEwan, I., Zhang,
723 A., Ashok, S., Rodgers, L., Russell, M., & Gately Luz, J. (2013). Structural context of
724 disease-associated mutations and putative mechanism of autoinhibition revealed by X-
725 ray crystallographic analysis of the EZH2-SET domain. *PLoS One, 8*(12), e84147.
726 https://doi.org/10.1371/journal.pone.0084147
727
728 Basheer, F., Giotopoulos, G., Meduri, E., Yun, H., Mazan, M., Sasca, D., Gallipoli, P., Marando, L.,
729 Gozdecka, M., Asby, R., Sheppard, O., Dudek, M., Bullinger, L., Dohner, H., Dillon, R.,
730 Freeman, S., Ottmann, O., Burnett, A., Russell, N., Papaemmanuil, E., Hills, R., Campbell,
731 P., Vassiliou, G. S., & Huntly, B. J. P. (2019, Apr 1). Contrasting requirements during
732 disease evolution identify EZH2 as a therapeutic target in AML. *J Exp Med, 216*(4), 966-
733 981. https://doi.org/10.1084/jem.20181276

Behringer, R., Gertsenstein, M., Nagy, K. V., & Nagy, A. (2016, Dec 1). Differentiating Mouse Embryonic Stem Cells into Embryoid Bodies by Hanging-Drop Cultures. *Cold Spring Harb Protoc, 2016*(12). https://doi.org/10.1101/pdb.prot092429

Beringer, M., Pisano, P., Di Carlo, V., Blanco, E., Chammas, P., Vizán, P., Gutiérrez, A., Aranda, S., Payer, B., Wierer, M., & Di Croce, L. (2016, Nov 17). EPOP Functionally Links Elongin and Polycomb in Pluripotent Stem Cells. *Mol Cell, 64*(4), 645-658. https://doi.org/10.1016/j.molcel.2016.10.018

Bernstein, E., Duncan, E. M., Masui, O., Gil, J., Heard, E., & Allis, C. D. (2006, Apr). Mouse polycomb proteins bind differentially to methylated histone H3 and RNA and are enriched in facultative heterochromatin. *Mol Cell Biol, 26*(7), 2560-2569. https://doi.org/10.1128/mcb.26.7.2560-2569.2006

Boheler, K. R., Czyz, J., Tweedie, D., Yang, H. T., Anisimov, S. V., & Wobus, A. M. (2002, Aug 9). Differentiation of pluripotent embryonic stem cells into cardiomyocytes. *Circ Res, 91*(3), 189-201. https://doi.org/10.1161/01.res.0000027865.61704.32

Bohm, J., Muenzner, J. K., Caliskan, A., Ndreshkjana, B., Erlenbach-Wunsch, K., Merkel, S., Croner, R., Rau, T. T., Geppert, C. I., Hartmann, A., Roehe, A. V., & Schneider-Stock, R. (2019, Sep). Loss of enhancer of zeste homologue 2 (EZH2) at tumor invasion front is correlated with higher aggressiveness in colorectal cancer cells. *J Cancer Res Clin Oncol, 145*(9), 2227-2240. https://doi.org/10.1007/s00432-019-02977-1

Bowman, S. K., Simon, M. D., Deaton, A. M., Tolstorukov, M., Borowsky, M. L., & Kingston, R. E. (2013, Jul 9). Multiplexed Illumina sequencing libraries from picogram quantities of DNA. *BMC Genomics, 14*, 466. https://doi.org/10.1186/1471-2164-14-466

Bradley, W. D., Arora, S., Busby, J., Balasubramanian, S., Gehling, V. S., Nasveschuk, C. G., Vaswani, R. G., Yuan, C. C., Hatton, C., Zhao, F., Williamson, K. E., Iyer, P., Méndez, J., Campbell, R., Cantone, N., Garapaty-Rao, S., Audia, J. E., Cook, A. S., Dakin, L. A., Albrecht, B. K., Harmange, J. C., Daniels, D. L., Cummings, R. T., Bryant, B. M., Normant, E., & Trojer, P. (2014, Nov 20). EZH2 inhibitor efficacy in non-Hodgkin's lymphoma does not require suppression of H3K27 monomethylation. *Chem Biol, 21*(11), 1463-1475. https://doi.org/10.1016/j.chembiol.2014.09.017

Bremer, S. C. B., Conradi, L. C., Mechie, N. C., Amanzada, A., Mavropoulou, E., Kitz, J., Ghadimi, M., Ellenrieder, V., Strobel, P., Hessmann, E., Gaedcke, J., & Bohnenberger, H. (2019, Nov 6). Enhancer of Zeste Homolog 2 in Colorectal Cancer Development and Progression. *Digestion*, 1-9. https://doi.org/10.1159/000504093

776 Chamberlain, S. J., Yee, D., & Magnuson, T. (2008, Jun). Polycomb repressive complex 2 is
777 dispensable for maintenance of embryonic stem cell pluripotency. *Stem Cells, 26*(6),
778 1496-1505. https://doi.org/10.1634/stemcells.2008-0102
779
780 Collinson, A., Collier, A. J., Morgan, N. P., Sienerth, A. R., Chandra, T., Andrews, S., & Rugg-Gunn,
781 P. J. (2016, Dec 6). Deletion of the Polycomb-Group Protein EZH2 Leads to Compromised
782 Self-Renewal and Differentiation Defects in Human Embryonic Stem Cells. *Cell Rep,*
783 *17*(10), 2700-2714. https://doi.org/10.1016/j.celrep.2016.11.032
784
785 Cyrus, S., Burkardt, D., Weaver, D. D., & Gibson, W. T. (2019, Dec). PRC2-complex related
786 dysfunction in overgrowth syndromes: A review of EZH2, EED, and SUZ12 and their
787 syndromic phenotypes. *Am J Med Genet C Semin Med Genet, 181*(4), 519-531.
788 https://doi.org/10.1002/ajmg.c.31754
789
790 Dang, S. M., Kyba, M., Perlingeiro, R., Daley, G. Q., & Zandstra, P. W. (2002, May 20). Efficiency
791 of embryoid body formation and hematopoietic development from embryonic stem
792 cells in different culture systems. *Biotechnol Bioeng, 78*(4), 442-453.
793 https://doi.org/10.1002/bit.10220
794
795 Deng, Y., Chen, X., Huang, C., Chen, G., Chen, F., Lu, J., Shi, X., He, C., Zeng, Z., Qiu, Y., Chen, J.,
796 Lin, R., Chen, Y., & Chen, J. (2019). EZH2/Bcl-2 Coexpression Predicts Worse Survival in
797 Diffuse Large B-cell Lymphomas and Demonstrates Poor Efficacy to Rituximab in
798 Localized Lesions. *J Cancer, 10*(9), 2006-2017. https://doi.org/10.7150/jca.29807
799
800 Dessau, R. B., & Pipper, C. B. (2008, Jan 28). ["R"--project for statistical computing]. *Ugeskr*
801 *Laeger, 170*(5), 328-330. (R--en programpakke til statistisk databehandling og grafik.)
802
803 Dobin, A., Davis, C. A., Schlesinger, F., Drenkow, J., Zaleski, C., Jha, S., Batut, P., Chaisson, M., &
804 Gingeras, T. R. (2013, Jan 1). STAR: ultrafast universal RNA-seq aligner. *Bioinformatics,*
805 *29*(1), 15-21. https://doi.org/10.1093/bioinformatics/bts635
806
807 Dou, D., Ge, X., Wang, X., Xu, X., Zhang, Z., Seng, J., Cao, Z., Gu, Y., & Han, M. (2019). EZH2
808 Contributes To Cisplatin Resistance In Breast Cancer By Epigenetically Suppressing miR-
809 381 Expression. *Onco Targets Ther, 12*, 9627-9637. https://doi.org/10.2147/ott.S214104
810
811 Ferguson, J., Devarajan, M., DiNuoscio, G., Saiakhova, A., Liu, C. F., Lefebvre, V., Scacheri, P. C.,
812 & Atit, R. P. (2018, Feb 2). PRC2 Is Dispensable in Vivo for β-Catenin-Mediated
813 Repression of Chondrogenesis in the Mouse Embryonic Cranial Mesenchyme. *G3*
814 *(Bethesda), 8*(2), 491-503. https://doi.org/10.1534/g3.117.300311
815
816 Fioravanti, R., Stazi, G., Zwergel, C., Valente, S., & Mai, A. (2018, Dec). Six Years (2012-2018) of
817 Researches on Catalytic EZH2 Inhibitors: The Boom of the 2-Pyridone Compounds. *Chem*
818 *Rec, 18*(12), 1818-1832. https://doi.org/10.1002/tcr.201800091
819

820 Fraineau, S., Palii, C. G., McNeill, B., Ritso, M., Shelley, W. C., Prasain, N., Chu, A., Vion, E., Rieck,
821 K., Nilufar, S., Perkins, T. J., Rudnicki, M. A., Allan, D. S., Yoder, M. C., Suuronen, E. J., &
822 Brand, M. (2017, Nov 14). Epigenetic Activation of Pro-angiogenic Signaling Pathways in
823 Human Endothelial Progenitors Increases Vasculogenesis. *Stem Cell Reports, 9*(5), 1573-
824 1587. https://doi.org/10.1016/j.stemcr.2017.09.009
825
826 Harris, J. (2018). Partial Clinical Hold on Tazemetostat Trials Lifted by FDA [News article].
827 *Targeted Oncology*.
828
829 Healy, E., Mucha, M., Glancy, E., Fitzpatrick, D. J., Conway, E., Neikes, H. K., Monger, C., Van
830 Mierlo, G., Baltissen, M. P., Koseki, Y., Vermeulen, M., Koseki, H., & Bracken, A. P. (2019,
831 Nov 7). PRC2.1 and PRC2.2 Synergize to Coordinate H3K27 Trimethylation. *Mol Cell,*
832 *76*(3), 437-452.e436. https://doi.org/10.1016/j.molcel.2019.08.012
833
834 Heinz, S., Benner, C., Spann, N., Bertolino, E., Lin, Y. C., Laslo, P., Cheng, J. X., Murre, C., Singh,
835 H., & Glass, C. K. (2010, May 28). Simple combinations of lineage-determining
836 transcription factors prime cis-regulatory elements required for macrophage and B cell
837 identities. *Mol Cell, 38*(4), 576-589. https://doi.org/10.1016/j.molcel.2010.05.004
838
839 Hescheler, J., Fleischmann, B. K., Lentini, S., Maltsev, V. A., Rohwedel, J., Wobus, A. M., &
840 Addicks, K. (1997, Nov). Embryonic stem cells: a model to study structural and functional
841 properties in cardiomyogenesis. *Cardiovasc Res, 36*(2), 149-162.
842 https://doi.org/10.1016/s0008-6363(97)00193-4
843
844 Hon, G. C., Song, C. X., Du, T., Jin, F., Selvaraj, S., Lee, A. Y., Yen, C. A., Ye, Z., Mao, S. Q., Wang,
845 B. A., Kuan, S., Edsall, L. E., Zhao, B. S., Xu, G. L., He, C., & Ren, B. (2014, Oct 23). 5mC
846 oxidation by Tet2 modulates enhancer activity and timing of transcriptome
847 reprogramming during differentiation. *Mol Cell, 56*(2), 286-297.
848 https://doi.org/10.1016/j.molcel.2014.08.026
849
850 Hunt, S. E., McLaren, W., Gil, L., Thormann, A., Schuilenburg, H., Sheppard, D., Parton, A.,
851 Armean, I. M., Trevanion, S. J., Flicek, P., & Cunningham, F. (2018, Jan 1). Ensembl
852 variation resources. *Database (Oxford), 2018*. https://doi.org/10.1093/database/bay119
853
854 Italiano, A., Soria, J. C., Toulmonde, M., Michot, J. M., Lucchesi, C., Varga, A., Coindre, J. M.,
855 Blakemore, S. J., Clawson, A., Suttle, B., McDonald, A. A., Woodruff, M., Ribich, S.,
856 Hedrick, E., Keilhack, H., Thomson, B., Owa, T., Copeland, R. A., Ho, P. T. C., & Ribrag, V.
857 (2018, May). Tazemetostat, an EZH2 inhibitor, in relapsed or refractory B-cell non-
858 Hodgkin lymphoma and advanced solid tumours: a first-in-human, open-label, phase 1
859 study. *Lancet Oncol, 19*(5), 649-659. https://doi.org/10.1016/s1470-2045(18)30145-1
860
861 Jain, P., & Di Croce, L. (2016, May). Mutations and deletions of PRC2 in prostate cancer.
862 *Bioessays, 38*(5), 446-454. https://doi.org/10.1002/bies.201500162
863

Juan, A. H., Wang, S., Ko, K. D., Zare, H., Tsai, P. F., Feng, X., Vivanco, K. O., Ascoli, A. M., Gutierrez-Cruz, G., Krebs, J., Sidoli, S., Knight, A. L., Pedersen, R. A., Garcia, B. A., Casellas, R., Zou, J., & Sartorelli, V. (2016, Oct 25). Roles of H3K27me2 and H3K27me3 Examined during Fate Specification of Embryonic Stem Cells. *Cell Rep, 17*(5), 1369-1382. https://doi.org/10.1016/j.celrep.2016.09.087

Karlowee, V., Amatya, V. J., Takayasu, T., Takano, M., Yonezawa, U., Takeshima, Y., Sugiyama, K., Kurisu, K., & Yamasaki, F. (2019). Immunostaining of Increased Expression of Enhancer of Zeste Homolog 2 (EZH2) in Diffuse Midline Glioma H3K27M-Mutant Patients with Poor Survival. *Pathobiology, 86*(2-3), 152-161. https://doi.org/10.1159/000496691

Kondo, Y. (2014, Nov). Targeting histone methyltransferase EZH2 as cancer treatment. *J Biochem, 156*(5), 249-257. https://doi.org/10.1093/jb/mvu054

Krill, L., Deng, W., Eskander, R., Mutch, D., Zweizig, S., Hoang, B., Ioffe, O., Randall, L., Lankes, H., Miller, D. S., & Birrer, M. (2020, Feb). Overexpression of enhance of Zeste homolog 2 (EZH2) in endometrial carcinoma: An NRG Oncology/Gynecologic Oncology Group Study. *Gynecol Oncol, 156*(2), 423-429. https://doi.org/10.1016/j.ygyno.2019.12.003

Lavarone, E., Barbieri, C. M., & Pasini, D. (2019, Apr 11). Dissecting the role of H3K27 acetylation and methylation in PRC2 mediated control of cellular identity. *Nat Commun, 10*(1), 1679. https://doi.org/10.1038/s41467-019-09624-w

Lewis, E., & Mislove, R. (1947). New mutants report. *Drosophila Information Service, 21*, 69.

Li, G., Margueron, R., Ku, M., Chambon, P., Bernstein, B. E., & Reinberg, D. (2010, Feb 15). Jarid2 and PRC2, partners in regulating gene expression. *Genes Dev, 24*(4), 368-380. https://doi.org/10.1101/gad.1886410

Li, H., Handsaker, B., Wysoker, A., Fennell, T., Ruan, J., Homer, N., Marth, G., Abecasis, G., & Durbin, R. (2009, Aug 15). The Sequence Alignment/Map format and SAMtools. *Bioinformatics, 25*(16), 2078-2079. https://doi.org/10.1093/bioinformatics/btp352

Liao, Y., Smyth, G. K., & Shi, W. (2014, Apr 1). featureCounts: an efficient general purpose program for assigning sequence reads to genomic features. *Bioinformatics, 30*(7), 923-930. https://doi.org/10.1093/bioinformatics/btt656

Liu, T. P., Lo, H. L., Wei, L. S., Hsiao, H. H., & Yang, P. M. (2015, Feb). S-Adenosyl-L-methionine-competitive inhibitors of the histone methyltransferase EZH2 induce autophagy and enhance drug sensitivity in cancer cells. *Anticancer Drugs, 26*(2), 139-147. https://doi.org/10.1097/cad.0000000000000166

907 Lue, J. K., & Amengual, J. E. (2018, Oct). Emerging EZH2 Inhibitors and Their Application in
908 Lymphoma. *Curr Hematol Malig Rep, 13*(5), 369-382. https://doi.org/10.1007/s11899-
909 018-0466-6
910
911 Margueron, R., Li, G., Sarma, K., Blais, A., Zavadil, J., Woodcock, C. L., Dynlacht, B. D., &
912 Reinberg, D. (2008, Nov 21). Ezh1 and Ezh2 maintain repressive chromatin through
913 different mechanisms. *Mol Cell, 32*(4), 503-518.
914 https://doi.org/10.1016/j.molcel.2008.11.004
915
916 Margueron, R., & Reinberg, D. (2011, Jan 20). The Polycomb complex PRC2 and its mark in life.
917 *Nature, 469*(7330), 343-349. https://doi.org/10.1038/nature09784
918
919 Matsubara, T., Toyokawa, G., Takada, K., Kinoshita, F., Kozuma, Y., Akamine, T., Shimokawa, M.,
920 Haro, A., Osoegawa, A., Tagawa, T., & Mori, M. (2019). The association and prognostic
921 impact of enhancer of zeste homologue 2 expression and epithelial-mesenchymal
922 transition in resected lung adenocarcinoma. *PLoS One, 14*(5), e0215103.
923 https://doi.org/10.1371/journal.pone.0215103
924
925 Mechaal, A., Menif, S., Abbes, S., & Safra, I. (2019, Sep). EZH2, new diagnosis and prognosis
926 marker in acute myeloid leukemia patients. *Adv Med Sci, 64*(2), 395-401.
927 https://doi.org/10.1016/j.advms.2019.07.002
928
929 Nakagawa, M., Koyanagi, M., Tanabe, K., Takahashi, K., Ichisaka, T., Aoi, T., Okita, K., Mochiduki,
930 Y., Takizawa, N., & Yamanaka, S. (2008, Jan). Generation of induced pluripotent stem
931 cells without Myc from mouse and human fibroblasts. *Nat Biotechnol, 26*(1), 101-106.
932 https://doi.org/10.1038/nbt1374
933
934 O'Geen, H., Ren, C., Nicolet, C. M., Perez, A. A., Halmai, J., Le, V. M., Mackay, J. P., Farnham, P.
935 J., & Segal, D. J. (2017, Sep 29). dCas9-based epigenome editing suggests acquisition of
936 histone methylation is not sufficient for target gene repression. *Nucleic Acids Res,*
937 *45*(17), 9901-9916. https://doi.org/10.1093/nar/gkx578
938
939 Pasini, D., Bracken, A. P., Hansen, J. B., Capillo, M., & Helin, K. (2007, May). The polycomb group
940 protein Suz12 is required for embryonic stem cell differentiation. *Mol Cell Biol, 27*(10),
941 3769-3779. https://doi.org/10.1128/mcb.01432-06
942
943 Pasini, D., Bracken, A. P., Jensen, M. R., Lazzerini Denchi, E., & Helin, K. (2004, Oct 13). Suz12 is
944 essential for mouse development and for EZH2 histone methyltransferase activity. *Embo*
945 *j, 23*(20), 4061-4071. https://doi.org/10.1038/sj.emboj.7600402
946
947 Pereira, C. F., Piccolo, F. M., Tsubouchi, T., Sauer, S., Ryan, N. K., Bruno, L., Landeira, D., Santos,
948 J., Banito, A., Gil, J., Koseki, H., Merkenschlager, M., & Fisher, A. G. (2010, Jun 4). ESCs
949 require PRC2 to direct the successful reprogramming of differentiated cells toward
950 pluripotency. *Cell Stem Cell, 6*(6), 547-556. https://doi.org/10.1016/j.stem.2010.04.013

Qi, W., Chan, H., Teng, L., Li, L., Chuai, S., Zhang, R., Zeng, J., Li, M., Fan, H., Lin, Y., Gu, J., Ardayfio, O., Zhang, J. H., Yan, X., Fang, J., Mi, Y., Zhang, M., Zhou, T., Feng, G., Chen, Z., Li, G., Yang, T., Zhao, K., Liu, X., Yu, Z., Lu, C. X., Atadja, P., & Li, E. (2012, Dec 26). Selective inhibition of Ezh2 by a small molecule inhibitor blocks tumor cells proliferation. *Proc Natl Acad Sci U S A, 109*(52), 21360-21365. https://doi.org/10.1073/pnas.1210371110

Rai, A. N., Vargas, M. L., Wang, L., Andersen, E. F., Miller, E. L., & Simon, J. A. (2013, Dec). Elements of the polycomb repressor SU(Z)12 needed for histone H3-K27 methylation, the interface with E(Z), and in vivo function. *Mol Cell Biol, 33*(24), 4844-4856. https://doi.org/10.1128/mcb.00307-13

Ramírez, F., Dündar, F., Diehl, S., Grüning, B. A., & Manke, T. (2014, Jul). deepTools: a flexible platform for exploring deep-sequencing data. *Nucleic Acids Res, 42*(Web Server issue), W187-191. https://doi.org/10.1093/nar/gku365

Robinson, J. T., Thorvaldsdóttir, H., Winckler, W., Guttman, M., Lander, E. S., Getz, G., & Mesirov, J. P. (2011, Jan). Integrative genomics viewer. *Nat Biotechnol, 29*(1), 24-26. https://doi.org/10.1038/nbt.1754

Robinson, M. D., McCarthy, D. J., & Smyth, G. K. (2010, Jan 1). edgeR: a Bioconductor package for differential expression analysis of digital gene expression data. *Bioinformatics, 26*(1), 139-140. https://doi.org/10.1093/bioinformatics/btp616

Schuettengruber, B., Bourbon, H. M., Di Croce, L., & Cavalli, G. (2017, Sep 21). Genome Regulation by Polycomb and Trithorax: 70 Years and Counting. *Cell, 171*(1), 34-57. https://doi.org/10.1016/j.cell.2017.08.002

Shan, Y., Liang, Z., Xing, Q., Zhang, T., Wang, B., Tian, S., Huang, W., Zhang, Y., Yao, J., Zhu, Y., Huang, K., Liu, Y., Wang, X., Chen, Q., Zhang, J., Shang, B., Li, S., Shi, X., Liao, B., Zhang, C., Lai, K., Zhong, X., Shu, X., Wang, J., Yao, H., Chen, J., Pei, D., & Pan, G. (2017, Sep 22). PRC2 specifies ectoderm lineages and maintains pluripotency in primed but not naïve ESCs. *Nat Commun, 8*(1), 672. https://doi.org/10.1038/s41467-017-00668-4

Shen, X., Kim, W., Fujiwara, Y., Simon, M. D., Liu, Y., Mysliwiec, M. R., Yuan, G. C., Lee, Y., & Orkin, S. H. (2009, Dec 24). Jumonji modulates polycomb activity and self-renewal versus differentiation of stem cells. *Cell, 139*(7), 1303-1314. https://doi.org/10.1016/j.cell.2009.12.003

Shen, X., Liu, Y., Hsu, Y. J., Fujiwara, Y., Kim, J., Mao, X., Yuan, G. C., & Orkin, S. H. (2008, Nov 21). EZH1 mediates methylation on histone H3 lysine 27 and complements EZH2 in maintaining stem cell identity and executing pluripotency. *Mol Cell, 32*(4), 491-502. https://doi.org/10.1016/j.molcel.2008.10.016

995
996 Shi, B., Behrens, C., Vaghani, V., Riquelme, E. M., Rodriguez-Canales, J., Kadara, H., Lin, H., Lee,
997 J., Liu, H., Wistuba, I., & Simon, G. (2019, Oct). Oncogenic enhancer of zeste homolog 2
998 is an actionable target in patients with non-small cell lung cancer. *Cancer Med, 8*(14),
999 6383-6392. https://doi.org/10.1002/cam4.1855
1000
1001 Skene, P. J., & Henikoff, S. (2017, Jan 16). An efficient targeted nuclease strategy for high-
1002 resolution mapping of DNA binding sites. *Elife, 6*. https://doi.org/10.7554/eLife.21856
1003
1004 Takahashi, K., & Yamanaka, S. (2006, Aug 25). Induction of pluripotent stem cells from mouse
1005 embryonic and adult fibroblast cultures by defined factors. *Cell, 126*(4), 663-676.
1006 https://doi.org/10.1016/j.cell.2006.07.024
1007
1008 Thornton, S. R., Butty, V. L., Levine, S. S., & Boyer, L. A. (2014). Polycomb Repressive Complex 2
1009 regulates lineage fidelity during embryonic stem cell differentiation. *PLoS One, 9*(10),
1010 e110498. https://doi.org/10.1371/journal.pone.0110498
1011
1012 Tian, Z., Li, Z., Zhu, Y., Meng, L., Liu, F., Sang, M., & Wang, G. (2019, Aug). Hypermethylation-
1013 mediated inactivation of miR-124 predicts poor prognosis and promotes tumor growth
1014 at least partially through targeting EZH2/H3K27me3 in ESCC. *Clin Exp Metastasis, 36*(4),
1015 381-391. https://doi.org/10.1007/s10585-019-09974-1
1016
1017 van Mierlo, G., Veenstra, G. J. C., Vermeulen, M., & Marks, H. (2019, Aug). The Complexity of
1018 PRC2 Subcomplexes. *Trends Cell Biol, 29*(8), 660-671.
1019 https://doi.org/10.1016/j.tcb.2019.05.004
1020
1021 Wasenang, W., Puapairoj, A., Settasatian, C., Proungvitaya, S., & Limpaiboon, T. (2019, Jul).
1022 Overexpression of polycomb repressive complex 2 key components EZH2/SUZ12/EED as
1023 an unfavorable prognostic marker in cholangiocarcinoma. *Pathol Res Pract, 215*(7),
1024 152451. https://doi.org/10.1016/j.prp.2019.152451
1025
1026 Wassef, M., Luscan, A., Aflaki, S., Zielinski, D., Jansen, P., Baymaz, H. I., Battistella, A., Kersouani,
1027 C., Servant, N., Wallace, M. R., Romero, P., Kosmider, O., Just, P. A., Hivelin, M., Jacques,
1028 S., Vincent-Salomon, A., Vermeulen, M., Vidaud, M., Pasmant, E., & Margueron, R.
1029 (2019, Mar 26). EZH1/2 function mostly within canonical PRC2 and exhibit proliferation-
1030 dependent redundancy that shapes mutational signatures in cancer. *Proc Natl Acad Sci*
1031 *U S A, 116*(13), 6075-6080. https://doi.org/10.1073/pnas.1814634116
1032
1033 Wu, X., Scott, H., Carlsson, S. V., Sjoberg, D. D., Cerundolo, L., Lilja, H., Prevo, R., Rieunier, G.,
1034 Macaulay, V., Higgins, G. S., Verrill, C. L., Lamb, A. D., Cunliffe, V. T., Bountra, C., Hamdy,
1035 F. C., & Bryant, R. J. (2019, Jul). Increased EZH2 expression in prostate cancer is
1036 associated with metastatic recurrence following external beam radiotherapy. *Prostate,*
1037 *79*(10), 1079-1089. https://doi.org/10.1002/pros.23817
1038

1039 Xu, B., On, D. M., Ma, A., Parton, T., Konze, K. D., Pattenden, S. G., Allison, D. F., Cai, L.,
1040 Rockowitz, S., Liu, S., Liu, Y., Li, F., Vedadi, M., Frye, S. V., Garcia, B. A., Zheng, D., Jin, J.,
1041 & Wang, G. G. (2015, Jan 8). Selective inhibition of EZH2 and EZH1 enzymatic activity by
1042 a small molecule suppresses MLL-rearranged leukemia. *Blood, 125*(2), 346-357.
1043 https://doi.org/10.1182/blood-2014-06-581082
1044
1045 Xu, H., Zhang, L., Qian, X., Zhou, X., Yan, Y., Zhou, J., Ge, W., Albahde, M., & Wang, W. (2019,
1046 Oct). GSK343 induces autophagy and downregulates the AKT/mTOR signaling pathway
1047 in pancreatic cancer cells. *Exp Ther Med, 18*(4), 2608-2616.
1048 https://doi.org/10.3892/etm.2019.7845
1049
1050 Yamagishi, M., & Uchimaru, K. (2017, Sep). Targeting EZH2 in cancer therapy. *Curr Opin Oncol,*
1051 *29*(5), 375-381. https://doi.org/10.1097/cco.0000000000000390
1052
1053 Yang, P. M., Hong, Y. H., Hsu, K. C., & Liu, T. P. (2019). p38α/S1P/SREBP2 activation by the SAM-
1054 competitive EZH2 inhibitor GSK343 limits its anticancer activity but creates a druggable
1055 vulnerability in hepatocellular carcinoma. *Am J Cancer Res, 9*(10), 2120-2139.
1056
1057 Yu, W., Zhang, F., Wang, S., Fu, Y., Chen, J., Liang, X., Le, H., Pu, W. T., & Zhang, B. (2017, Apr
1058 13). Depletion of polycomb repressive complex 2 core component EED impairs fetal
1059 hematopoiesis. *Cell Death Dis, 8*(4), e2744. https://doi.org/10.1038/cddis.2017.163
1060
1061 Zhang, M. J., Chen, D. S., Li, H., Liu, W. W., Han, G. Y., & Han, Y. F. (2019). Clinical significance of
1062 USP7 and EZH2 in predicting prognosis of laryngeal squamous cell carcinoma and their
1063 possible functional mechanism. *Int J Clin Exp Pathol, 12*(6), 2184-2194.
1064
1065 Zhang, Q., Han, Q., Zi, J., Ma, J., Song, H., Tian, Y., McGrath, M., Song, C., & Ge, Z. (2019, Sep).
1066 Mutations in EZH2 are associated with poor prognosis for patients with myeloid
1067 neoplasms. *Genes Dis, 6*(3), 276-281. https://doi.org/10.1016/j.gendis.2019.05.001
1068
1069